The Term Structure of Interest Rates in a Heterogeneous Monetary Union*

James Costain, Galo Nuño, and Carlos Thomas
Banco de España

May 2022

Abstract

We build a no-arbitrage model of the yield curves in a heterogeneous monetary union with sovereign default risk, which can account for the asymmetric shifts in euro area yields during the Covid-19 pandemic. We derive an affine term structure solution, and decompose yields into term premium and credit risk components. In an extension, we endogenize the peripheral default probability, showing that it decreases with central bank bond-holdings. Calibrating the model to Germany and Italy, we show that a "default risk extraction" channel is the main driver of Italian yields, and that flexibility makes asset purchases more effective.

Keywords: sovereign default, quantitative easing, yield curve, affine model, Covid-19 crisis, ECB, pandemic emergency purchase programme.

JEL classification: E5, G12, F45.

*This draft replaces an earlier version entitled "Assessing the effectiveness of the ECB's pandemic purchase program: a term structure modelling approach". The views expressed in this manuscript are those of the authors and do not necessarily represent the views of Banco de España or the Eurosystem. The authors are grateful for helpful comments from Valery Charnavoki, Ricardo Gimeno, Thomas King, Wolfgang Lemke, Bartosz Mackowiak, Dimitros Malliaropulos, Ken Nyholm, Walker Ray, Ricardo Reis, Jean-Paul Renne, Dominik Thaler, and an anonymous referee, and also from seminar participants at the ECB, the Banco de España, the 3rd Spanish Macroeconomics Network workshop, the 24th Central Bank Macroeconomic Modelling Workshop, the 3rd ILMA conference (HSE Moscow), the Banque de France - CEPR meeting on "Monetary Policy, Fiscal Policy, and Public Debt in a Post COVID world", and at the 2021 meetings of the SCE, CEBRA, and EEA. All remaining errors are ours.

1 Introduction

The sovereign yield curve – also known as the "term structure of interest rates" – is a crucial indicator of financing conditions for any given country. Central banks pay great attention to the yield curve(s) under their jurisdiction, since they constitute a key channel of monetary policy transmission, and also provide relevant information about the shocks hitting the economy. The importance of yield curves for monetary policy analysis has only increased since the Great Financial Crisis of 2008-09: as (short-term) policy rates in advanced economies approached their effective lower bounds, central banks resorted to unconventional tools, such as large-scale asset purchases and forward guidance about future short rates, in order to flatten the yield curve and thus provide further policy stimulus.

In this context, term structure models have become important analytical tools, both for central bankers and for scholars of monetary policy. In particular, they underlie the prevailing view of the effects of asset purchase programmes, which revolves around the "duration risk extraction" channel (*e.g.* Greenwood and Vayanos, 2014; Hamilton and Wu, 2012; or Krishnamurthy, 2022). Under this mechanism, net purchases of long-maturity bonds flatten the yield curve by reducing the term premium that private markets demand to compensate for duration risk, while the short end of the curve is anchored by the risk-free short rate. However, the movements of euro area yield curves (see Figure 1) in response to the pandemic outbreak in early 2020 and to the ECB's subsequent monetary policy response challenge this view. While duration extraction might explain the flattening of the German yield curve after the pandemic emergency purchase programme (PEPP) announcement on March 18, 2020, it offers no explanation of the much larger movements in the Italian and Spanish yield curves. A key feature of these movements is the large shift in the short end of the peripheral curves, which cannot be explained by term premium considerations. The same is true for the large upward shift in peripheral yield curves as the pandemic shock unfolded (before PEPP was announced), which cannot be explained by invoking the pandemic's impact on the expected amount of duration risk to be absorbed by the market.

It is not hard to see why the mainstream view of term structure dynamics fails to explain yields in southern Europe, when we consider that today's workhorse models, such as the influential Vayanos and Vila (2020) framework, abstract from sovereign default risk. While it may be reasonable to assume that there is no nominal default

Figure 1: Effects of the pandemic and the PEPP announcement on German, Spanish, and Italian yields

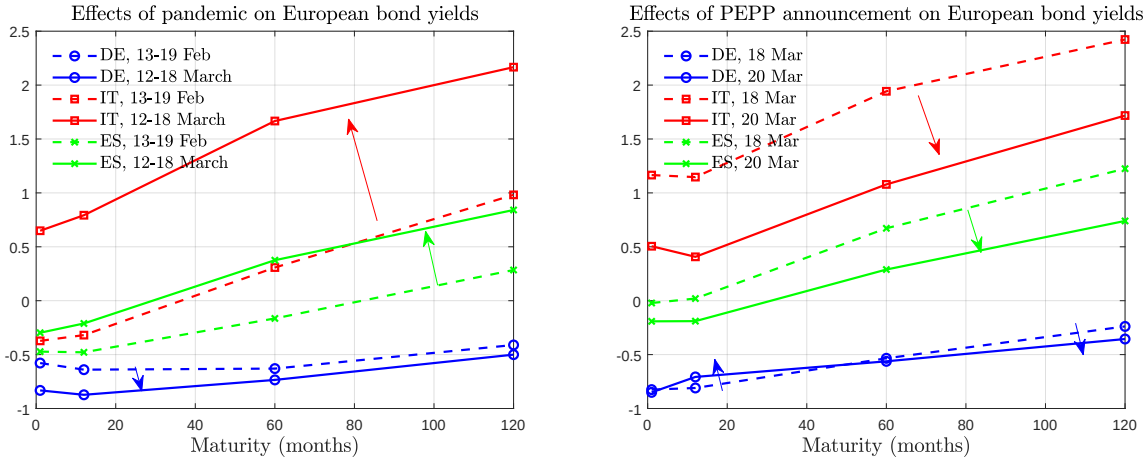

Notes. Data source: Datastream.
Left panel. Shifts in German, Spanish, and Italian zero-coupon yields (annual percentage points) from the weekly average of 13-19 Feb. 2020 (dashes), to that of 12-18 Mar. 2020 (solid).
Right panel. Shifts in German, Spanish, and Italian zero-coupon yields (annual percentage points) from 18 March 2020 (dashes, before PEPP announcement) to 20 March 2020 (solid, after).

risk on the debt of the safest issuers, such as the US Treasury, such an abstraction is less suitable for the euro area, where sovereign issuers that are viewed as safe coexist – and share a common monetary policy – with other issuers that face high and volatile credit risk premia. Sovereign credit risk offers a possible explanation for the nearly mirror-image dynamics of European yield curves in response to the pandemic outbreak and the PEPP announcement, if we view these not as two qualitatively different shocks, but as two impulses that each affect yields through changes, of opposite sign, in the probability of default.

Motivated by these observations, this paper proposes a micro-founded model of the term structure of sovereign interest rates designed to address a heterogeneous monetary union such as the euro area. To do so, we extend the Vayanos and Vila (2020) term structure model to a multi-country setting with sovereign default risk. Concretely, we consider a monetary union consisting of two member states: Core, which issues default-free bonds, and Periphery, which is subject to default risk. The model is populated by arbitrageurs, who trade bonds across both countries and all maturities, and preferred-habitat investors, who demand bonds of a specific maturity from a specific jurisdiction.

Bond yields in the model are driven by just one stochastic factor, namely the short-term riskless rate.[1] Yields also depend on the *net* supply of bonds of each maturity and jurisdiction, by which we mean bond supply from the governments minus the bonds held by the common monetary authority. For analytical convenience, we treat the governments' bond supply and central bank bond demand as deterministic sequences; this may be interpreted as a situation in which the public sector commits to a particular time path for the net supply of bonds in the market.

We start by analyzing a model version with an exogenous default arrival probability, following Duffie and Singleton (1999), which is useful for two reasons. First, it shows how the affine solution of the Vayanos and Vila (2020) model generalizes in the presence of default risk. Second, it highlights key results that are independent of how one models the probability of sovereign default. In particular, our solution decomposes bond yields into four components: (i) an *expectations* term that represents the expected future path of the risk-free rate; (ii) a *term premium* representing the risk-averse compensation for bearing duration risk; (iii) an *expected default loss*, which captures the compensation that a risk-neutral investor would require for holding defaultable bonds; and (iv) a *credit risk premium* that represents the risk-averse compensation for absorbing default risk (over and above expected default losses). Thus, while many analyses of asset purchase programs emphasize the duration extraction channel, our model distinguishes this from a *default risk extraction channel* that operates through the credit risk premium rather than the term premium: risk-averse investors demand less compensation to hold a defaultable bond when there is less default risk outstanding in the market. Moreover, we show that the presence of default risk allows for shifts in the front end of the yield curve in response to shocks that cause the default probability to vary but have otherwise no effect on short-term riskless rates.

While imposing an exogenous default probability simplifies and clarifies the analysis, in reality large-scale asset purchase shocks like the PEPP announcement, or other shocks with fiscal implications, such as the pandemic outbreak, are likely to affect the default probability perceived by markets. Therefore, we next extend the model by linking the default probability to underlying policy choices. To do so, we assume that the peripheral bond market is subject to rollover crises in the spirit of Calvo (1988) and Cole and Kehoe (2000). When a rollover crisis arrives, the peripheral fiscal authority decides whether to

[1] Although this is a one-factor model, it can be easily extended to a multifactor environment. The multifactor case is documented in the help files for our simulation programs.

continue servicing its debts or else to partially default by applying a haircut to bonds of all maturities. We show that, under certain conditions, the peripheral government's default probability at any given time depends on the present discounted value of the future expected path of fiscal deficits plus redemptions of privately-held bonds. This is because redemptions of bonds held by the central bank (or interest payments on those bonds) represent payments from the treasury to the central bank which will be rebated back to the treasury through central bank dividends. Therefore, by purchasing sovereign bonds, the central bank reduces the fiscal pressure that the peripheral government will face if a rollover crisis arrives, and thus reduces its incentives to default, a point made by Corsetti and Dedola (2016).[2] By contrast, when bonds remain in private hands, they imply a net repayment obligation for the government, making default more likely. Crucially, all results obtained from the exogenous default probability case carry through to the endogenous case. However, endogenizing the default probability reinforces the yield curve impact of asset purchases, both because purchases decrease the expected default loss and – more importantly – because the default risk extraction channel is stronger when asset purchases *both* reduce the net supply of defaultable bonds *and* reduce the default risk on each bond.

To evaluate the model's ability to explain how euro area yields reacted to the PEPP, and to quantify the importance of the different transmission channels, we calibrate our model to Germany and Italy. The calibration uses yield curve data from the years before the pandemic, and also from the two-day window around the ECB's initial PEPP announcement on March 18, 2020, which declared an aggregate purchase envelope of 750 billion euros. The surprise nature of this announcement, in an emergency meeting of the ECB Governing Council, makes it easy to map this episode into our model. The calibration revolves around three key parameters: arbitrageurs' risk aversion is identified by matching the pre-pandemic German term premium; the expected loss due to default is identified from the pre-pandemic spread on Italian bonds over German bonds; and the impact of net bond issuance on the default probability is identified by explaining the fall in Italian yields when PEPP was announced. Given the relatively high degree of risk aversion needed to explain the German term premium, only a tiny expected default

[2]We implicitly assume the existence of national central banks that conduct asset purchases on behalf of the union-wide central bank. This is broadly consistent with Eurosystem practice, where the large majority of purchases are actually conducted by national central banks, instead of the ECB. Under this assumption, it is indeed the consolidated budget constraint of each country's fiscal authority and national central bank that matters for the former's default incentives.

loss is needed to explain the observed spread on Italian debt. Despite its parsimony, our model replicates well the average pre-pandemic shape of both countries' yield curves, as well as their asymmetric immediate reaction to the PEPP announcement, including the large downward shift of the Italian curve.

Decomposing the movements of the yield curves, we find that default risk extraction is the most significant channel – far more relevant than the fall in term premia – to explain the behavior of yields in our model. It is particularly important for the shape of the response of the Italian yield curve to the PEPP announcement, and for the asymmetry of the responses of the German and Italian curves. The downward shift in the Italian sovereign spread, across all maturities, is explained almost entirely by a lower credit risk premium, driven both by a small decline in the probability of peripheral default and by the reduction in the quantity of defaultable assets that the market was expected to hold from then on. In contrast, the decrease in the expected loss due to default, by itself, plays only a small role in reducing the sovereign spread. These results are in line with the empirical evidence put forward by Corradin et al. (2021) for the same episode, which concludes that a reduction in default risk was the dominant channel through which the PEPP announcement operated in the case of Italy; likewise they are consistent with findings of Krishnamurthy et al. (2018) and **?** regarding earlier asset purchase programs in Europe.

Our quantitative, structural model also allows us to construct counterfactual scenarios to compare PEPP with other possible asset purchase designs. To ensure an adequate response to the asymmetric impact of the Covid-19 shock, PEPP was designed to be *flexible* in the distribution of purchases over time, across asset classes, and across euro area jurisdictions. This flexibility contrasted with the ECB's longer-standing Asset Purchase Programme (APP), which fixed the pace of purchases over time, and allocated purchases across member states by their "capital keys" – i.e., in proportion to the share of each Eurosystem national central bank in the ECB's capital. Our simulations show that PEPP's flexible design substantially enhanced its impact, and that flexibility in the timing of purchases (frontloading) and flexibility in the allocation across countries (deviations from capital key) complement and reinforce one another. The PEPP announcement reduced Italian yields by around 80bp across the yield curve, with its maximal impact at intermediate maturities. Of this overall effect, almost 15bp can be attributed to the flexibility of PEPP, as compared with a counterfactual program under which a constant rate of purchases would be allocated across countries according to

capital key. Moreover, flexibility matters for the response of *average* euro-area yields, because reallocation towards peripheral bonds has a large impact on peripheral yields but a negligible impact on those of core bonds.

Related literature. This paper links two different strands of literature. First, we contribute to the finance literature on term structure models. In liquid markets, arbitrage links bond returns tightly across maturities and issuers. Ang and Piazzesi (2003), building on Duffie and Kan (1996), derived an analytical solution for the yield curve in the absence of arbitrage opportunities under the assumption that all yields are affine functions of a set of autoregressive Gaussian factors. Vayanos and Vila (2020) showed that an affine term structure model (ATSM) of this type applies to a micro-founded setting featuring arbitrageurs with mean-variance utility functions, together with "preferred-habitat" investors whose supply or demand for bonds of specific maturities is linear in those bonds' yields. This market structure makes it possible to model a variety of complex bond market interactions and policy interventions. For example, Greenwood and Vayanos (2014) offered empirical support for the model's prediction that the price of risk increases as arbitrageurs hold larger maturity-weighted positions; therefore quantitative easing can reduce yields, even if the face value of debt outstanding is unchanged. Further applications include quantitative easing at the effective lower bound (Hamilton and Wu, 2012; King, 2019), repo market dynamics (He et al., 2020), and exchange rates (Greenwood et al., 2020; Gourinchas et al., 2020). The bond market structure of Vayanos and Vila (2020) has also been embedded into a New Keynesian model to analyze monetary policy in general equilibrium (Ray 2019). Motivated by the theoretical insights of Vayanos and Vila (2020), various papers have incorporated net supply factors into otherwise standard no-arbitrage ATSMs, including Li and Wei (2013) and Eser et al. (2019); the latter paper uses security-level data on sectoral bond holdings to construct a measure of duration risk in the hands of price-sensitive investors (akin to Vayanos and Vila's arbitrageurs) and to analyze the impact of the APP.

While they have been widely applied, much of the literature using ATSMs has studied US markets, under the assumption that Treasury securities are nominally riskless. Applications to fixed exchange rate environments – including monetary unions – or to commercial debt make it necessary to consider default risk. Hamilton and Wu (2012) construct an ATSM that includes one-period defaultable non-Treasury debt. A key insight about defaultable bond prices comes from Duffie and Singleton (1999), who show that if the loss caused by default is a fixed fraction of the bond's value, then the

pricing formulas for default-free and defaultable bonds are formally identical, with an adjustment to the discount factor to account for expected losses due to default. Borgy et al. (2012) price defaultable euro-area debt under the assumption that the Duffie and Singleton (1999) condition holds. Altavilla et al. (2021) modelled euro area debt under the assumption that default risk can be priced like any other Gaussian factor.

We contribute to this literature in several ways. We show how the non-Gaussian risk of default – specifically, partial default on multi-period debt – can be incorporated into a microfounded ATSM in the Vayanos-Vila tradition. Crucially, we show that default risk opens up a novel *default risk extraction channel* of large-scale asset purchases, which enables the model to generate large, parallel yield curve shifts like those in Figure 1. In addition, we adapt the model to analyze policy interactions in the context of a heterogeneous monetary union, such as the euro area. Finally, we model explicitly how central bank asset purchases affect the default probability by incorporating the possibility of rollover crises, showing how this reinforces the default risk extraction channel *vis-à-vis* the simpler case with exogenous default probability. This mechanism can be seen as an extension of the two-period economy of Corsetti and Dedola (2016) to a fully dynamic environment.

This paper also relates to the literature on monetary-fiscal interactions in the presence of sovereign risk.[3] In contrast to previous related work, we focus on how central bank asset purchases can reduce the probability of default, and how they affect the whole term structure of interest rates. Linking the ATSM literature to that on sovereign risk is fruitful, because it clarifies that duration extraction is neither the only channel, nor the primary channel, by which asset purchases transmit to yields in the European context. Instead, our model shows that default risk extraction is the predominant channel of asset purchases in the euro area, as the extraction of defaultable bonds from private hands and the associated reduction in the probability of sovereign default reinforce one another in shrinking the credit risk premium. The quantitative discipline of the ATSM framework is crucial here – arbitrage pricing implies that the actual expected loss from default is an order of magnitude smaller than the risk premium that the market demands to hold defaultable debt. The channel we identify is consistent with evidence of De Grauwe and Ji (2013) showing that sovereign spreads are less stable in the euro

[3]See Calvo (1988), Cole and Kehoe (2000), Aguiar et al. (2015), Reis (2013), Corsetti and Dedola (2016), Camous and Cooper (2019), Bacchetta et al. (2018), Nuño et al. (2022), Na et al. (2018), Arellano et al. (2020), or Bianchi and Mondragon (2018).

area than in other open economies with independent monetary policies, and findings of Broeders et al. (2021) showing that ECB asset purchases reduced the impact of bond market volatility on euro area sovereign spreads.

2 Bond market equilibrium with default risk

We begin by building a model of bond market equilibrium that incorporates an exogenous but time-varying probability of partial default. This simple version of our model shows how introducing default risk in a Vayanos-Vila framework that is entirely standard – apart from its two-country monetary union structure – modifies the bond market equilibrium and shapes the transmission of central bank asset purchases, without taking a stance on the modelling of sovereign default. Subsequently, we will extend the model to include a monetary/fiscal interactions block that endogenizes the default probability.

Time is continuous, with an infinite horizon. We consider a monetary union composed of two countries, Core and Periphery, with a single central bank. The key difference between the two governments is that Core issues risk-free debt whereas Periphery may default on its obligations. We denote Core variables with an asterisk, $'*'$. There exists a continuum of zero-coupon government bonds of different maturities. The time-t price of a bond with maturity τ is $P_t(\tau)$ for Peripheral bonds and $P_t^*(\tau)$ for Core bonds. The *yield* is the spot rate for maturity τ :

$$y_t(\tau) = -\frac{\log P_t(\tau)}{\tau}, \quad y_t^*(\tau) = -\frac{\log P_t^*(\tau)}{\tau} \ .$$

We assume that default follows a Poisson stochastic process, as in Duffie and Singleton (1999). Let ψ_t be the arrival rate of sovereign default by the government of Periphery. While it is easy to allow for default by both sovereigns, for clarity we focus on the case where the probability of Core default is zero. Peripheral default, when it occurs, consists of a restructuring in which the government reneges on fraction δ of its outstanding bonds. Default affects all maturities of Peripheral debt equally.

There exists a short-term (instantaneous) riskless interest rate which is exogenous and characterized by an Ornstein–Uhlenbeck process,

$$dr_t = \kappa(\bar{r} - r_t)\,dt + \sigma dB_t, \tag{1}$$

where B_t is a Brownian motion and κ and $\bar{r}$ are constants. The short-term riskless rate and the default shock itself are the only stochastic processes in this economy. The Peripheral default arrival rate ψ_t is deterministic but may depend on time.[4]

Net bond supply. The public sector of the monetary union determines the net supply of bonds, consisting of the gross supply issued by the Peripheral and Core governments minus the bonds held by the common central bank. Let $f_t(\tau)$ be the stock of Peripheral sovereign debt of maturity τ outstanding at time t, and let $\iota_t(\tau)$ represent the rate of issuance of bonds of this type per unit of time. Then the law of motion of the stock of Peripheral debt is

$$\frac{\partial f_t(\tau)}{\partial t} = \iota_t(\tau) + \frac{\partial f_t(\tau)}{\partial \tau}, \tag{2}$$

which implies that the quantity of bonds of residual maturity τ outstanding at time t, $f_t(\tau)$, equals the current gross issuance of bonds of that maturity, $\iota_t(\tau)\,dt$, plus the stock of bonds of maturity $\tau + dt$ that was outstanding at time $t - dt$. The dynamics of the Core debt stock $f_t^*(\tau)$, given issuances $\iota_t^*(\tau)$, are formally identical to (2). Likewise, the central bank purchases $\iota_t^{CB}(\tau)$ bonds of maturity τ from Periphery per unit of time, resulting in a Peripheral portfolio $f_t^{CB}(\tau)$ that evolves as

$$\frac{\partial f_t^{CB}(\tau)}{\partial t} = \iota_t^{CB}(\tau) + \frac{\partial f_t^{CB}(\tau)}{\partial \tau}, \tag{3}$$

with analogous dynamics for its portfolio of Core bonds. We denote the net supplies of Periphery and Core bonds by

$$S_t(\tau) \equiv f_t(\tau) - f_t^{CB}(\tau), \quad S_t^*(\tau) \equiv f_t^*(\tau) - f_t^{CB*}(\tau),$$

respectively. For ease of exposition, but without loss of generality, we assume that net bond supplies are deterministic but possibly time-varying functions.[5]

Bond demand. We consider two classes of private agents that demand bonds. *Preferred-habitat investors* demand bonds of a specific jurisdiction and specific maturity, as an increasing function of the bonds' yield. Market participants with these char-

[4]The assumption that ψ_t is deterministic is essential in order to obtain an affine solution, as we will see below.

[5]The model in this section can be extended to allow for stochastic net bond supply, by including a stochastic shift in equation (4), as in Vayanos and Vila (2020), but this is not needed for our purposes.

acteristics may include pension funds or insurance companies whose liability streams require them to hold assets paying off at specific times in the distant future, or money-market mutual funds that must hold assets that provide liquidity at short horizons. *Arbitrageurs* are willing to hold bonds of any maturity and jurisdiction, and may also invest in the riskless short rate, but their positions are limited by their risk aversion. These players represent liquid, well-informed market participants, such as hedge funds, which nonetheless are unwilling to take arbitrarily large risks.

As in Vayanos and Vila (2020) we assume that preferred-habitat investors' demand for bonds of a given jurisdiction and maturity increases with the yield on those bonds:

$$Z_t(\tau) = h_t(\tau) - \alpha(\tau)\log P_t(\tau), \quad Z_t^*(\tau) = h_t^*(\tau) - \alpha^*(\tau)\log P_t^*(\tau), \tag{4}$$

where $\alpha(\tau), \alpha^*(\tau) \geq 0$ and $h_t(\tau), h_t^*(\tau)$ are deterministic functions.[6]

The main focus of our analysis is the arbitrageurs, who maximize a mean-variance objective over instantaneous changes in wealth, as in Vayanos and Vila (2020),

$$\max_{\{X_t(\tau), X_t^*(\tau)\}_{\tau\in(0,\infty)}} \mathbb{E}_t(dW_t) - \frac{\gamma}{2}\mathbb{V}ar_t(dW_t) \tag{5}$$

subject to the law of motion of wealth:

$$\begin{aligned} dW_t &= \left[W_t - \int_0^\infty \left(X_t(\tau) + X_t^*(\tau)\right) d\tau\right] r_t dt \\ &+ \int_0^\infty \left(X_t(\tau)\left(\frac{dP_t(\tau)}{P_t(\tau)} - \delta dN_t\right) + X_t^*(\tau)\frac{dP_t^*(\tau)}{P_t^*(\tau)}\right) d\tau, \end{aligned} \tag{6}$$

where $\gamma > 0$ is the representative arbitrageur's risk-aversion coefficient, and $X_t(\tau)$ and $X_t^*(\tau)$ are the nominal quantities of bonds of different maturities held in the arbitrageur's portfolio. The first term in (6) shows the income from investing in the short-term riskless rate, while the second term shows the capital gains from holding a portfolio of Peripheral bonds $X_t(\tau)$ and Core bonds $X_t^*(\tau)$, adjusted for the possible arrival of the default event according to a Poisson process dN_t. Note that arbitrageurs can operate in both markets (Core and Periphery), similar to Gourinchas et al. (2020).

Bond market clearing. Bond market clearing requires consistency between supply

[6] We set $\alpha(\tau) = \alpha(\tau)^* = \alpha/\tau$. Thus, the slope of preferred-habitat demand, as a function of yield, is given by the constant α: $Z_t(\tau) = h_t + \alpha y_t(\tau)$, and analogously for $Z_t^*(\tau)$.

and demand for bonds of each maturity and jurisdiction:

$$S_t(\tau) = Z_t(\tau) + X_t(\tau), \quad S_t^*(\tau) = Z_t^*(\tau) + X_t^*(\tau) \ . \tag{7}$$

That is, net supply by the public sector equals demand by preferred-habitat investors plus that of arbitrageurs.

Bond pricing. We assume that after default, the Peripheral government issues new bonds to replace the defaulted bonds, thus returning to its initial deterministic path of gross bond supply.[7] Thus, default leaves the state of the bond market unchanged, so we seek to construct an equilibrium in which bond prices do not depend on previous default events. We conjecture that there exist two pairs of deterministic functions $(A_t(\tau), C_t(\tau))$ and $(A_t^*(\tau), C_t^*(\tau))$ such that the price of bonds can be expressed in log-affine form:

$$P_t(\tau) = e^{-[A_t(\tau) r_t + C_t(\tau)]}, \ P_t^*(\tau) = e^{-[A_t^*(\tau) r_t + C_t^*(\tau)]}. \tag{8}$$

Applying Itô's lemma, the time-t instantaneous return on an undefaulted bond of maturity τ is

$$\frac{dP_t(\tau)}{P_t(\tau)} = \mu_t(\tau)\, dt - \sigma A_t(\tau)\, dB_t, \ \frac{dP_t^*(\tau)}{P_t^*(\tau)} = \mu_t^*(\tau)\, dt - \sigma A_t^*(\tau)\, dB_t, \tag{9}$$

where[8]

$$\mu_t(\tau) = \left(\frac{\partial A_t}{\partial \tau} - \frac{\partial A_t}{\partial t}\right) r_t + \left(\frac{\partial C_t}{\partial \tau} - \frac{\partial C_t}{\partial t}\right) - A_t(\tau)\,\kappa(\bar{r} - r_t) + \frac{1}{2}\sigma^2 [A_t(\tau)]^2, \tag{10}$$

and

$$\mu_t^*(\tau) = \left(\frac{\partial A_t^*}{\partial \tau} - \frac{\partial A_t^*}{\partial t}\right) r_t + \left(\frac{\partial C_t^*}{\partial \tau} - \frac{\partial C_t^*}{\partial t}\right) - A_t^*(\tau)\,\kappa(\bar{r} - r_t) + \frac{1}{2}\sigma^2 [A_t^*(\tau)]^2. \tag{11}$$

[7] Perhaps surprisingly, it would be unrealistic to suppose that debt decreases when default occurs. On the contrary, Arellano et al. (2019) show that debt is more likely to *increase* following a restructuring. As in their paper, the model of monetary/fiscal interactions that we develop in Section 3 implies that default serves to alleviate short-term fiscal pressure, not to reduce the debt load permanently.

[8] Note that τ is a state with dynamics $d\tau = -dt$, so Itô's lemma yields derivatives in τ as well as t.

If we substitute bond returns (9) into the law of motion of wealth (6), we obtain

$$\begin{aligned} dW_t &= \left[W_t r_t + \int_0^\infty \left(X_t(\tau)\left(\mu_t(\tau) - r_t\right) + X_t^*(\tau)\left(\mu_t^*(\tau) - r_t\right)\right) d\tau\right] dt \\ &- \left[\int_0^\infty \left(X_t(\tau) A_t(\tau) + X_t^*(\tau) A_t^*(\tau)\right) d\tau\right] \sigma dB_t \\ &- \left[\int_0^\infty X_t(\tau)\, d\tau\right] \delta dN_t. \end{aligned} \tag{12}$$

Thus, wealth is affected by two different types of risk: a Brownian variation in bond prices (seen in the second line of the formula), together with a Poisson risk of losing a fraction δ of the investment in Peripheral bonds (third line). Using equation (12) in (5), one can see that the problem of the arbitrageurs accounts for both these risks:

$$\begin{aligned} \max_{\{X_t(\tau), X_t^*(\tau)\}_{\tau\in(0,\infty)}} & \int_0^\infty \left(X_t(\tau)\left(\mu_t(\tau) - r_t\right) + X_t^*(\tau)\left(\mu_t^*(\tau) - r_t\right)\right) d\tau \\ - & \frac{\gamma\sigma^2}{2}\left[\int_0^\infty \left(X_t(\tau) A_t(\tau) + X_t^*(\tau) A_t^*(\tau)\right) d\tau\right]^2 \\ - & \psi_t \delta \left[\int_0^\infty X_t(\tau)\, d\tau\right] \\ - & \frac{\gamma\psi_t}{2}\delta^2 \left[\int_0^\infty X_t(\tau)\, d\tau\right]^2. \end{aligned}$$

The first two terms represent the expectation and variance of the component associated with price variation, while the last two terms are derived from default risk, using $\mathbb{E}\left[\delta dN_t\right] = \delta\psi_t$ and $\mathbb{V}ar\left[\delta dN_t\right] = \delta^2\psi_t$.

The first-order conditions are

$$\mu_t(\tau) = r_t + A_t(\tau)\lambda_t + \psi_t\delta + \xi_t, \tag{13}$$

$$\mu_t^*(\tau) = r_t + A_t^*(\tau)\lambda_t, \tag{14}$$

where[9]

$$\lambda_t = \gamma\sigma^2\left[\int_0^\infty \left(X_t(\tau) A_t(\tau) + X_t^*(\tau) A_t^*(\tau)\right) d\tau\right] \tag{15}$$

is the *market price of (interest rate) risk* and

$$\xi_t = \gamma\psi_t\delta^2 \int_0^\infty X_t(\tau)\, d\tau \tag{16}$$

[9]Our notation in this section follows Vayanos and Vila (2020), except that we have reversed the sign on the variables λ and h.

is the compensation required by risk-averse arbitrageurs for *default risk*. Equation (14) shows that the expected growth rate of Core bond prices equals the short-term riskless rate of return, r_t, plus the compensation $A_t^*(\tau)\lambda_t$ for the instantaneous price risk on a bond of a given maturity τ. Analogous terms apply to the expected growth of Peripheral bond prices, given by (13), plus the compensation $\psi_t\delta$ for the rate of expected loss due to default, together with the instantaneous default risk premium ξ_t.

Constructing an affine solution. Market clearing (7) requires that the positions of arbitrageurs equal those of the public sector minus those of the preferred-habitat investors. Using this in equations (15) and (16), the risk prices λ_t and ξ_t must satisfy:

$$\lambda_t = \gamma\sigma^2 \left[\int_0^\infty \left[\left(S_t(\tau) - Z_t(\tau) \right) A_t(\tau) + \left(S_t^*(\tau) - Z_t^*(\tau) \right) A_t^*(\tau) \right] d\tau \right], \tag{17}$$

$$\xi_t = \gamma\psi_t\delta^2 \int_0^\infty \left(S_t(\tau) - Z_t(\tau) \right) d\tau. \tag{18}$$

Equations (17)-(18) can be used to solve for the unknown coefficients $A_t(\tau)$, $A_t^*(\tau)$, $C_t(\tau)$, and $C_t^*(\tau)$ in the bond price functions (see Appendix A.2). The solution hinges on the observation that if ψ_t is a deterministic function of time, then the left- and right-hand sides of (18) can both be affine functions of r_t (since preferred-habitat demand Z is affine in r).[10] In this case, we can construct an affine solution (8) for prices and yields, in which the risk prices λ_t and ξ_t are also affine:

$$\lambda_t = \Lambda_t r_t + \bar{\lambda}_t, \tag{19}$$

$$\xi_t = \Xi_t r_t + \bar{\xi}_t. \tag{20}$$

Appendix A.2 spells out the affine solution in detail, stating the formulas for the factor loadings Λ_t and Ξ_t and intercept terms $\bar{\lambda}_t$ and $\bar{\xi}_t$ consistent with (17)-(18).

2.1 Equilibrium yield curves and monetary policy transmission: analytical results

Our model's analytical solution provides insight into yield curve dynamics and the transmission of conventional and unconventional monetary policy. Here we discuss four

[10] If instead ψ_t is a stochastic process that depends on r_t, then there are nonlinear terms on the right-hand side of (18), so the affine solution fails.

main findings. First, we decompose yields to distinguish the familiar *expectations* and *duration extraction* transmission channels of asset purchase policy from our model's novel *default risk extraction channel*, which arises when debt is defaultable. Second, we show how, when the default probability is small, the term premium in the yield curves of both Core and Periphery depends on the *aggregate* net bond supply in the monetary union, irrespective of its distribution across countries. Third, we show that default risk allows for heterogeneous fluctuations in short-term sovereign rates in a monetary union, including shifts in the short end of the Peripheral yield curve even when the short-term riskless rate does not change. Finally, we show that conventional interest rate policy transmits homogeneously across a monetary union, limiting its scope for stabilizing asymmetric fluctuations.

Decomposing bond yields. In the absence of default risk, equations (10)-(11) and (13)-(14) imply identical yield curves for Core and Periphery. But when Peripheral bonds are defaultable, this opens up a spread relative to Core bonds. Taking expectations on both sides of (9), then using (13) and the fact that $P_t(0) = 1$, we can decompose the yield on a Peripheral bond of maturity τ as follows.[11]

Proposition 1 (Bond yield decomposition) *Peripheral yields $y_t(\tau)$ can be written as*

$$\begin{aligned} y_t(\tau) &= \underbrace{\frac{1}{\tau}\mathbb{E}_t\int_0^\tau r_{t+s}ds}_{\text{Expected rates } y_t^{EX}(\tau)} + \underbrace{\frac{1}{\tau}\mathbb{E}_t\int_0^\tau A_{t+s}(\tau-s)\lambda_{t+s}ds}_{\text{Term premium } y_t^{TP}(\tau)} \\ &+ \underbrace{\frac{1}{\tau}\mathbb{E}_t\int_0^\tau \delta\psi_{t+s}ds}_{\text{Expected default loss } y_t^{DL}(\tau)} + \underbrace{\frac{1}{\tau}\mathbb{E}_t\int_0^\tau \xi_{t+s}ds}_{\text{Credit risk premium } y_t^{CR}(\tau)}. \end{aligned} \tag{23}$$

For the proof, see Appendix A.3.1. Thus, Peripheral yields decompose into four

[11] Equivalently, the bond price can be written as a product of log-affine factors:

$$P_t(\tau) = P_t^{EX}(\tau)P_t^{TP}(\tau)P_t^{DL}(\tau)P_t^{CR}(\tau) \tag{21}$$
$$P_t^*(\tau) = P_t^{EX*}(\tau)P_t^{TP*}(\tau) \tag{22}$$

where, for each $i \in \{EX, TP, DL, CR\}$, we have $P_t^i(\tau) = \exp\left(-\tau y_t^i(\tau)\right)$, and likewise for Core.

affine components. The default-related components are zero for Core:

$$y_t(\tau) = y_t^{EX}(\tau) + y_t^{TP}(\tau) + y_t^{DL}(\tau) + y_t^{CR}(\tau), \tag{24}$$

$$y_t^*(\tau) = y_t^{EX*}(\tau) + y_t^{TP*}(\tau). \tag{25}$$

The first component, which is equalized across countries, $y_t^{EX}(\tau) = y_t^{EX*}(\tau)$, is the yield in a default-free economy where investors are risk neutral. This is often called the *expected rates term*, since it is the yield in a default-free economy where the "expectations hypothesis" is true: that is, the bond yield equals the expected value of the short rate over the life of the bond. The second component is the *term premium*, that is, the compensation required by a risk-averse arbitrageur for holding a bond with a risky price. Since the price process of a defaultable bond differs from that of a default-free bond, the Core and Peripheral term premia, $y_t^{TP*}(\tau)$ and $y_t^{TP}(\tau)$, are not exactly equal. The third component, in the case of Peripheral bonds, is the *expected default loss* $y_t^{DL}(\tau)$, which requires compensation even for a risk-neutral investor. Fourth, the yield on Peripheral bonds also carries a *credit risk premium* $y_t^{CR}(\tau)$, which is the additional return required, beyond the expected default loss, in order for a risk-averse arbitrageur to be willing to hold a defaultable bond. Together, the two components $y_t^{DL}(\tau) + y_t^{CR}(\tau)$, plus the cross-country difference in term premia $y_t^{TP}(\tau) - y_t^{TP*}(\tau)$, constitute the (sovereign) spread between Peripheral and Core debt.

This decomposition highlights four different channels of monetary policy transmission. First, policy transmits through anticipated changes in the future path of interest rates (e.g. due to forward guidance). Second, it operates through *duration extraction*, by which central bank bond purchases reduce the market price of interest rate risk, as in the one-factor version of Vayanos and Vila (2020). Third, policy transmits through changes in the expected default loss, as central bank purchases may reduce the likelihood of sovereign default, as explained in Section 3 below. Finally, it transmits through *default risk extraction*, as we can see by using (18) to write the credit risk premium as

$$y_t^{CR}(\tau) = \frac{\gamma\delta^2}{\tau}\mathbb{E}_t \int_0^\tau \left[\psi_{t+s} \int_0^\infty \left(S_{t+s}(\tau) - Z_{t+s}(\tau)\right) d\tau\right] ds \ .$$

This shows that central bank bond purchases reduce credit risk premia, both by extracting defaultable debt $S_{t+s}(\tau)$ from the market, and – once it is allowed to depend on central bank purchases – by lowering the probability of default ψ_{t+s} on that debt.

Term premium in a monetary union. While our decomposition highlights a new transmission channel going through credit risk, our model also delivers basic insights about the transmission of asset purchases via term premia in a monetary union. For simplicity, but without loss of generality, we focus on the model's stochastic steady state, in which the short rate r_t is stochastic, but there is no further time variation in the model's parameters. We suppress time subscripts wherever possible when analyzing the stochastic steady state. As shown in Appendix A.3.2, in the stochastic steady state the coefficients $A_t(\tau)$ and $A_t^*(\tau)$ are given by

$$A^*(\tau) = \frac{1-e^{-\hat{\kappa}\tau}}{\hat{\kappa}},\ A(\tau) = \frac{(1+\Xi)\left(1-e^{-\hat{\kappa}\tau}\right)}{\hat{\kappa}}, \tag{26}$$

where

$$\hat{\kappa} = \kappa - \Lambda = \kappa + \gamma\sigma^2 \int_0^\infty \left(\alpha(\tau) \left(\frac{(1+\Xi)\left(1-e^{-\hat{\kappa}\tau}\right)}{\hat{\kappa}} \right)^2 + \alpha^*(\tau) \left(\frac{1-e^{-\hat{\kappa}\tau}}{\hat{\kappa}} \right)^2 \right) d\tau,$$

is the risk-neutral counterpart of κ, and $\Xi = -\gamma\psi\delta^2 \int_0^\infty \alpha(\tau) A(\tau) d\tau < 0$ is the steady state value of the loading of the default risk price ξ_t on the short rate (eq. 20). We then obtain the following result:

Proposition 2 (Term premia in a monetary union with low default risk) *Let the default probability ψ be arbitrarily close to zero, $\psi \to 0$, so that $\Xi \to 0$. In this limiting case, $A(\tau) = A^*(\tau)$. Term premia are then equalized across the two countries:*

$$y_t^{TP}(\tau) = \frac{1}{\tau}\mathbb{E}_t \int_0^\tau A(\tau - s)\lambda_{t+s} ds = y_t^{TP*}(\tau),$$

and the market price of duration risk depends on the aggregate net bond supply in the monetary union:

$$\lambda_t = \gamma\sigma^2 \int_0^\infty \underbrace{\left[\left(S(\tau) + S^*(\tau) \right) - \left(Z_t(\tau) + Z_t^*(\tau) \right) \right]}_{\textit{aggregate net bond supply}} A(\tau) d\tau.$$

A policy implication of this result is that, when default risk is arbitrarily small, asset purchases affect Core and Peripheral term premia symmetrically, and this effect depends only on the *aggregate* amount of purchases and not on how they are distributed across

jurisdictions. This benchmark will be helpful in interpreting our subsequent numerical results, since our calibrated default probability turns out to be fairly small.

What drives the short end of the yield curve? For a country without default risk, the shortest maturity yield coincides with the short-term riskless rate:

$$\begin{aligned}\lim_{\tau\to 0} y_t^*(\tau) &= \lim_{\tau\to 0}\left[\frac{1}{\tau}\mathbb{E}_t\int_0^\tau r_{t+s}ds + \frac{1}{\tau}\mathbb{E}_t\int_0^\tau A_{t+s}^*(\tau-s)\lambda_{t+s}ds\right]\\ &= \lim_{\tau\to 0}\left[r_t + A_t^*(0)\lambda_t\right] = r_t,\end{aligned}$$

where the second equality applies L'Hôpital's rule and the Leibniz rule and the fact that $A_t^*(0) = 0$. Therefore, in the absence of default risk, changes in structural parameters can produce changes in the slope of the yield curve, but the short end of the curve is pinned down to equal the short-term rate.[12]

Hence, if we abstract from default, our model cannot reproduce yield curve shifts like those observed in Europe in the context of Covid-19 and the PEPP announcement (see Figure 1 above). But once we allow for default risk, parallel shifts are possible, even in the absence of changes in the short-term riskless rate.

Proposition 3 (Default risk-related shifts in the Peripheral yield curve) *In a country with default risk, the yield curve in the stochastic steady state is the sum of a constant term that depends on default* $\left(\psi\delta + \bar{\xi}\right)$ *and a maturity-dependent affine term:*

$$\begin{aligned}y_t(\tau) &= \frac{A(\tau)r_t + C(\tau)}{\tau}\\ &= \left(\psi\delta + \bar{\xi}\right) + \frac{(1+\Xi)\left(1-e^{-\hat{\kappa}\tau}\right)}{\hat{\kappa}\tau}r_t + \frac{\int_0^\tau\left[A(u)\left(\kappa\bar{r}+\bar{\lambda}\right) - \frac{1}{2}\sigma^2\left[A(u)\right]^2\right]du}{\tau}.\end{aligned}$$

Therefore, the short-term Peripheral yield is given by

$$\lim_{\tau\to 0} y_t(\tau) = (1+\Xi)r_t + \left(\psi\delta + \bar{\xi}\right).$$

For proof details, see Appendix A.3.2. Note that the default-related term $\psi\delta + \bar{\xi}$ is independent of maturity τ, so this term produces a parallel shift in the yield curve when any of its components change. Hence, the possibility of default affects even the

[12] This result generalizes beyond the one-factor model considered here. Even in a multi-factor context, an instantaneous bond without default risk satisfies $A^*(0) = 0$ and $C^*(0) = 0$, implying $y_t^*(0) = r_t$. See Vayanos and Vila (2020), Lemma 3.

shortest yields, generating a spread between the shortest-maturity Peripheral yield and the risk-free short rate. The spread includes the expected default loss $\psi\delta$. The second term is the intercept $\bar{\xi}$ of the credit risk premium ξ from (20), which is

$$\bar{\xi} = \gamma\psi\delta^2 \int_0^\infty \left(S(\tau) - h(\tau) - \alpha(\tau) C(\tau)\right) d\tau. \tag{27}$$

Equation (27) shows that changes in the default arrival rate ψ, the haircut δ or the risk aversion parameter γ will, *ceteris paribus*, modify the credit risk premium and hence shift the Peripheral yield curve. Asset purchases will also shift Peripheral yields, including the shortest yields, by decreasing $\bar{\xi}$ through two channels. First, they extract default risk from arbitrageurs' balance sheets (reducing the quantity $S(\tau)$ that private markets must hold). Second, if asset purchases reduce the probability of default, this will amplify the decrease in $\bar{\xi}$. In the next section, we show how monetary and fiscal interactions like those in the euro area imply that central bank sovereign bond purchases reduce fiscal pressure, and thereby lower the probability of Peripheral default.

Conventional monetary policy transmission. Finally, we analyze how default risk shapes the transmission of conventional (interest rate) monetary policy across the monetary union. For the purpose of this particular discussion, we interpret r_t as representing the interest paid by the central bank on its deposit facility.[13] Concretely, as in Vayanos and Vila (2020), we may assume that arbitrageurs are actually commercial banks, with access to the central bank's deposit facility. We can then show:

Proposition 4 (Response to short-term rates) *The reaction of the instantaneous forward rate, $i_t(\tau) \equiv -\frac{\partial \log(P_t(\tau))}{\partial \tau}$, is identical in Core and Periphery:*

$$\frac{\partial i_t(\tau)}{\partial r_t} = -\frac{\partial}{\partial r_t}\frac{\partial \log\left(P_t(\tau)\right)}{\partial \tau} = e^{-\hat{\kappa}\tau} = \frac{\partial i_t^*(\tau)}{\partial r_t}.$$

If we instead consider the yield curve itself, then the initial response to a monetary policy shock at time t is:

$$\frac{\partial y_t^*(\tau)}{\partial r_t} = \frac{1 - e^{-\hat{\kappa}\tau}}{\tau\hat{\kappa}} > \frac{(1+\Xi)\left(1 - e^{-\hat{\kappa}\tau}\right)}{\tau\hat{\kappa}} = \frac{\partial y_t(\tau)}{\partial r_t}.$$

[13] This implies that the short-term Core yield, $\lim_{\tau\to 0} y_t^*(\tau)$, coincides with the deposit facility rate. Of course, this is not precisely true in the euro area data, where the yield on short-term core (e.g. German) bonds typically exhibits a non-negligible and time-varying spread vis-à-vis the ECB's deposit facility rate, reflecting institutional features that fall outside the scope of our analysis.

This response subsequently decays at rate κ with the time since the shock.

Since $\Xi < 0$ (see appendix A.2), the reaction of Peripheral yields is damped in comparison to that of Core yields. But in practice, the difference is negligible: if the default arrival rate ψ is sufficiently close to zero, then $\Xi \approx 0$, so the responses of the two yield curves are approximately equal. In the quantitative section below we will see that the data imply a small value for ψ. Hence our calibrated model implies that the impact of conventional monetary policy on Core and Peripheral yields is virtually indistinguishable.

3 A simple model of default risk

Thus far, we have treated the default arrival rate ψ_t as an arbitrary exogenous sequence. In practice, however, policy shocks like the PEPP announcement or the pandemic outbreak are likely to endogeneously affect the probability of default perceived by the market. Therefore, we next build a minimalist model of monetary and fiscal interactions that endogenizes ψ_t in a way that will suffice for our analysis of the yield curve. We assume that the governments and the monetary authorities commit to fixed time paths for their respective issuances and purchases of bonds, as long as no rollover crisis occurs. The one key policy choice that we will endogenize is Periphery's decision whether to repay or default in case of a rollover crisis.

The flow budget constraint of the Peripheral government can be written as

$$\overbrace{d_t}^{\text{Primary deficit}} + \overbrace{f_t(0)}^{\text{Debt maturing}} = \overbrace{\int_0^\infty P_t(\tau)\,\iota_t(\tau)\,d\tau}^{\text{Bond issuance}} + \overbrace{\Gamma_t}^{\text{Seigniorage}} + \overbrace{\Pi_t}^{\text{Emergency taxation}}, \tag{28}$$

where d_t is the primary deficit and $f_t(0)$ the amount of debt maturing, which must be financed either by issuing new bonds $\iota_t(\tau)$, collecting revenues from seigniorage Γ_t related to central-bank asset purchases, or through emergency taxation Π_t. Emergency taxation is zero in normal times, but may be positive during rollover crises.

Mirroring Corsetti and Dedola (2016), we focus on self-fulfilling debt crises *à la* Calvo (1988) or Cole and Kehoe (2000). We assume that investors sometimes, with a certain probability, coordinate on a pessimistic equilibrium in which they stop purchasing Periphery's debt, thus forcing its government to stop bond issuance ($\iota_t(\tau) = 0$,

for all τ).[14] The arrival of this rollover crisis is governed by a Poisson process with rate parameter η. At the onset of the crisis, the government must decide whether to default on its debts or to keep on repaying bonds that mature. If it decides to repay, the duration of the crisis is stochastic, governed by a Poisson process with parameter ϕ, and the government will be forced to finance its deficits and debt repayments with the revenues it obtains from emergency taxation and/or seigniorage as long as the crisis persists. Emergency taxes represent a utility loss for the government, which it seeks to minimize. Under these assumptions, the government's cost of repayment conditional on a rollover crisis at time 0, denoted by V_0^R, incorporates the present discounted value of emergency taxation incurred during the crisis, valued at a subjective discount rate $\hat{r}$, plus the continuation cost $V_t\left[f_t\left(\cdot\right), f_t^{CB}\left(\cdot\right)\right]$ after the crisis ends:

$$V_0^R\left[f_0\left(\cdot\right), f_0^{CB}\left(\cdot\right)\right] = \mathbb{E}_0\left\{\int_0^\infty e^{-(\hat{r}+\phi)t}\left(\underbrace{\Pi_t}_{\text{Flow of emergency taxes}} + \phi\underbrace{V_t\left[f_t\left(\cdot\right), f_t^{CB}\left(\cdot\right)\right]}_{\text{Loss after the crisis}}\right)dt\right\}. \tag{29}$$

If instead the government decides to default, it restructures by repudiating a fixed fraction δ of all outstanding bonds, while honoring the remainder. This restructuring ends the rollover crisis, but imposes a stochastic fixed cost χ on the government, with *c.d.f.* $\Phi(\chi)$. Thus, the loss due to default is the post-crisis continuation cost plus the fixed cost:

$$V_0^D\left[f_0\left(\cdot\right), f_0^{CB}\left(\cdot\right)\right] = V_0\left[f_0\left(\cdot\right), f_0^{CB}\left(\cdot\right)\right] + \chi. \tag{30}$$

Note that (30) says that default leaves the fiscal position of the government unchanged, with the same debts it faced before the crisis. While this may seem counterintuitive, we make this assumption for two reasons. First, it is empirically realistic: Arellano et al. (2019) show that debt is rarely decreased by a restructuring. Second, it simplifies our asset pricing analysis, keeping the outstanding bond supply fixed, allowing us to seek a bond price solution that is unchanged by default.[15] Thus, in our model, default

[14] We assume that the central bank cannot purchase sovereign new bonds at issuance, consistently with actual restrictions on the ECB's asset purchase programs. Thus, the fact that private investors stop purchasing new bonds effectively prevents the Peripheral government from issuing new bonds.

[15] Our interpretation of (30) is that after default, the Peripheral government immediately issues bonds that return it to the previously anticipated path of debt. Bondholders lose a fraction δ of their holdings, while the proceeds from the sale of new bonds accrue to international organizations, such as the IMF, that may intervene in the case of a sovereign debt crisis.

serves only to relieve short-term fiscal pressure during a rollover crisis, not to improve the government's long-term fiscal standing.

The government's decision to default at the beginning of a crisis will thus depend on $\min\left[V_0^R, V_0^D\right]$. The continuation cost is given by

$$V_0\left[f_0\left(\cdot\right), f_0^{CB}\left(\cdot\right)\right] = \mathbb{E}_0\left\{\int_0^\infty e^{-(\hat{r}+\eta)t} \underbrace{\eta \min\left[V_t^R, V_t^D\right]}_{\text{Loss at onset of next crisis}} dt\right\}. \tag{31}$$

Equations (29)-(31) jointly determine the loss functions V_t^R, V_t^D, and V_t. For simplicity, we focus on the limit where crises are low-probability events ($\eta \to 0$),[16] which means that the continuation cost is approximately zero, $V_t \to 0$, so that $V_0^D \to \chi$. Then the probability of default, conditional on a rollover crisis at time 0, is the probability that the cost of repayment exceeds the fixed cost χ:

$$\mathbb{P}\left(\text{default at time } 0|\text{crisis}\right) = \mathbb{P}\left(V_0^R > V_0^D\right) \approx \mathbb{P}\left(V_0^R > \chi\right) = \Phi\left(V_0^R\right). \tag{32}$$

Equations (32), (29) and (28), and the fact that there are no issuances during the rollover crisis ($\iota_t\left(\tau\right) = 0$ for all τ), imply that the *unconditional* arrival rate of default is $\psi_t = \eta\Phi_t$, where

$$\Phi_t \equiv \mathbb{P}\left(\text{default at time } t|\text{crisis}\right) = \Phi\left(\int_0^\infty e^{-(\hat{r}+\phi)s}\left\{d_{t+s} + f_{t+s}(0) - \Gamma_{t+s}\right\} ds\right). \tag{33}$$

Therefore, conditional on a rollover crisis materializing at time t, the probability that the government chooses to default increases with the discounted stream of primary deficits and bond redemptions during the crisis, and decreases with the discounted stream of remittances from the central bank during the crisis.

To evaluate expression (33), we must specify the central bank's seigniorage rule during a rollover crisis. It is plausible to conjecture that, should a full-blown rollover crisis hit a national government, the central bank would follow a rule under which an *increased* flow of central bank purchases of that government's bonds would *not* imply *less* resources for that government for the duration of the crisis.[17] We may refer to rules

[16] In our simulations of the effective lower bound period 2013-2019 in Section 4, the quantity $\psi_t \equiv \eta\Phi_t$ is never expected to exceed five basis points per month, so the assumption that η is tiny is reasonable.

[17] The central bank is assumed to stick to its bond purchase commitments when the private bond

of this kind as being *sovereign-supportive*. Formally, we define a sovereign-supportive rule $\Gamma_t = \Gamma\left(\left\{f^{CB}_{t+u}(\tau)\right\}_{u\geq 0,\tau\geq 0}\right)$ as a rule that, in a rollover crisis, satisfies:

$$\frac{\partial}{\partial\alpha}\left[\int_0^\infty e^{-(\hat{r}+\phi)u}\Gamma\left(\left\{f^{CB}_{t+u}(\tau)+\alpha h_{t+u}(\tau)\right\}_{u\geq 0,\tau\geq 0}\right)du\right]\geq 0, \tag{34}$$

where $h_{t+u}(\tau)\geq 0$ is a non-negative perturbation to the time-$(t+u)$ central bank holdings of Periphery bonds with residual maturity τ. That is, under a sovereign-supportive remittance rule, a central bank's decision to increase its future holdings of peripheral debt would not decrease the discounted stream of dividend payments to the peripheral government in case of – and for the duration of – a rollover crisis. It trivially follows that, for any rule satisfying this property, an increase in central bank purchases of peripheral bonds (weakly) *reduces* the endogenous default arrival rate.

Having established this general result, we still need to specify a particular crisis-time remittance rule for the purpose of our numerical analysis. We assume a tractable rule that corresponds roughly to actual Eurosystem practice. In particular, we assume the rule $\Gamma_t = f^{CB}_t(0) - \bar{\Gamma}$, meaning that the central bank rebates to the Peripheral government the inflows it receives from bond redemptions, minus an amount $\bar{\Gamma}$ aimed at protecting the central bank's capital during the rollover crisis. Currently, in the Eurosystem, most sovereign bonds are held by the national central banks of the sovereigns that issued them, with only a small fraction of holdings subject to "risk sharing". Therefore much of the income from sovereign bond redemptions accrues as dividend revenue to the original issuers. Thus, our key assumption here is simply that the central bank would not suddenly cut off this revenue flow upon the arrival of a rollover crisis. Moreover, the above rule can be shown to be "sovereign-supportive" as defined before.[18] The intuition is simple: increased central bank bond holdings lead to higher subsequent inflows from bond redemptions and thus higher remittances to Periphery's government. Therefore, increased purchases of Periphery bonds reduce that country's default rate.

---

market enters into a rollover crisis.

[18] Under the given rule, $\Gamma\left(\left\{f^{CB}_{t+u}(\tau)+\alpha h_{t+u}(\tau)\right\}_{u\geq 0,\tau\geq 0}\right) = f^{CB}_{t+u}(0)+\alpha h_{t+u}(0)-\bar{\Gamma}$. Therefore, $\frac{\partial\Gamma}{\partial\alpha} = \{h_{t+u}(0)\}_{u\geq 0}$, and hence the condition (34) is just $\int_0^\infty e^{-(\hat{r}+\phi)u}h_{t+u}(0)du\geq 0$, which is true since the perturbation h is non-negative.

Under our assumed remittance rule, the default rate is

$$\psi_t \quad = \quad \eta\Phi\left(\int_0^\infty e^{-(\hat{r}+\phi)s}\left\{d_{t+s}+S_{t+s}(0)+\bar{\Gamma}\right\}ds\right). \tag{35}$$

Equation (35) shows that the sovereign default probability depends on future deficits d_{t+s} at horizons $s \geq 0$, but it likewise implies that the central bank can affect the default probability via the future flow of redemptions of bonds in private hands, $S_{t+s}(0) = f_{t+s}(0) - f^{CB}_{t+s}(0)$. *Ceteris paribus*, if central bank policy reduces the amount of maturing public debt held by the private sector, the sovereign default probability will decrease. Under this remittance rule, we can calculate the default probability using only projections of future deficits and net redemptions, which affect the default probability through a single sufficient statistic which we will call *fiscal pressure*, F_t:

$$F_t \equiv \int_0^\infty e^{-(\hat{r}+\phi)s}\left(d_{t+s}+S_{t+s}\left(0\right)\right)ds, \tag{36}$$

so that $\psi_t = \eta\Phi\left(F_t + \frac{\bar{\Gamma}}{\hat{r}+\phi}\right)$.

This framework makes several stark assumptions which, together, deliver tractability. On one hand, we focus on perfect-foresight scenarios for fiscal policy and central bank purchases, assuming that the government returns to its previous path of debt after default occurs. Moreover, our assumed remittance rule ensures that the default probability depends only on deficits and net debt outstanding.[19] Together, these assumptions imply that fiscal pressure is foreseeable, so default is an event that arrives at a known, deterministic Poisson rate $\psi_t = \eta\Phi_t$. This means we can apply the framework of Duffie and Singleton (1999) to obtain an affine solution for the term structure and to decompose bond yields into components related to the dynamics of the risk-free rate and components related to default, as we described in Section 2.1.[20] Unanticipated changes in fiscal conditions will shift the default probability, with potential to explain the yield curve dynamics seen over the course of the Covid-19 crisis. We next calibrate

[19] Alternative remittance rules could include maintaining a constant level of central bank capital, or paying out the central bank's net cash flow. These rules would make remittances depend on the stock of central bank reserves. Such alternative rules are less tractable both because they imply additional state variables (e.g. the stock of reserves), and because the default probability will in general depend on the dynamics of future bond prices, implying an additional fixed point loop in the solution. See Appendix A.1 for a discussion of the dynamics of the central bank's reserves and capital.

[20] As we saw earlier, our affine solution fails when the default probability itself is stochastic.

our model to perform a quantitative evaluation of the PEPP announcement, which then provides a basis for counterfactual analysis of alternative asset purchase policies.

4 Quantitative analysis

4.1 Calibration: pre-pandemic conditions

We calibrate the model under the assumption that the two countries in the union, Core and Periphery, represent Germany and Italy, respectively, and we interpret the risk-free short rate r_t as the yield on one-month German sovereign bonds.[21] The yield curve decomposition (24)-(25) suggests a clear set of empirical targets to identify the three key model parameters. First, (17) implies that the German term premium is increasing in the risk aversion parameter γ. Second, for any γ, the sovereign premium on Italian debt will increase with the probability of default, ψ_t. We will target the German yield curve and the Italian sovereign premium under pre-pandemic conditions, which we take to mean the period 2013-2019 in which the ECB policy rate remained close to the effective lower bound, or "ELB period" for brevity. Third, the impact of the PEPP announcement on Italian yields will depend on the slope of the default probability with respect to fiscal pressure, $\frac{\partial \psi}{\partial F} = \eta \frac{\partial \Phi}{\partial F}$. We will jointly estimate γ, and the level and slope of ψ_t, conditional on a value of the preferred-habitat slope, $\alpha = 500$, which fits the data well. The asset purchase effects we identify are largely unaffected by α, over a wide range of possible values of this parameter.[22]

Interest rate data. We will evaluate our model by comparing it to monthly data from Datastream on zero-coupon German and Italian sovereign yields at one-month, one-year, five-year and ten-year maturities. To identify the model parameters we must also calibrate the stochastic factor that drives yields, namely, the risk-free rate r_t. For consistency with pre-pandemic conditions, we set the standard deviation of r_t to $\sigma_{elb} =$ 32bp, which is the sample standard deviation of the one-month German zero-coupon rate over 2013-2019.[23] We set the long-run value of the short-term riskless rate to

[21] Similar results are obtained if we calibrate to Germany and Spain instead. See Appendix B.

[22] The precise value of α is not crucial for our results, as long as preferred-habitat demand is not too elastic. A highly elastic specification is rejected, because it implies that yields are no longer monotonically decreasing with purchases. Illustrative simulations are available upon request.

[23] We use the subscript "elb" to denote sample and model moments over the ELB period.

$\bar{r} = 1\%$, which is consistent with long-run expectations in the ECB's Survey of Monetary Analysts (SMA).[24] In other words, the ELB period can indeed be characterized as a prolonged deviation from the expected long-run level of eurozone interest rates.[25] Lastly, we set the autocorrelation of r_t by matching the anticipated half-life of its deviation from its long-run value, as observed in the SMA. This leads us to set the monthly autocorrelation of r_t at 0.992, or equivalently $\kappa = 0.096$.

Fiscal pressure. Yields during the ELB period will also depend on market participants' expectations about fiscal trends at that time. As regards gross bond supply, we calibrate expectations using ECB/Eurosystem quarterly projections, from 2013 to 2019 vintages, of German and Italian general government debt securities over a ten year horizon.[26] Regarding bond absorption, we construct ten-year-ahead projections of Eurosystem asset purchases based on ECB announcements and analysts' expectations on APP purchases reported in Bloomberg surveys.[27] We interpolate the forecasts to monthly frequency, and we assume for simplicity that bonds are issued with maturities from one month to ten years, and that the stock of bonds is uniform across maturities.[28] Under these assumptions, we can calculate the anticipated net supplies of German and Italian bonds, $f^*_{t+s}(\tau) - f^{CB,*}_{t+s}(\tau)$ and $f_{t+s}(\tau) - f^{CB}_{t+s}(\tau)$ for each forecast vintage t, each forecast horizon s, and each maturity τ – including $\tau = 0$, which gives us net bond redemptions. We average over vintages t to obtain an average net supply forecast for the ELB period, at all horizons s.

Likewise, we can aggregate forward to calculate fiscal pressure.[29] For time aggrega-

[24] The ECB started conducting the SMA in March 2019. In the six surveys conducted in 2019, the year before the pandemic, the median (across surveyed analysts) long-run expectation for euro area short-term riskless rates averaged 1.08%, and stood at 1% in the last four rounds. The results from the SMA have been published since June 2021 and are available here.

[25] Alternatively, we could allow for regime shifts, regarding the ELB period as one possible regime, and calibrate the model to fit that regime, setting the mean and standard deviation of r_t to $r_{elb} = -49$bp and $\sigma_{elb} = 32$bp. This procedure gives similar results, as we show in Appendix B.

[26] Debt is assumed constant after the last forecasted value. The same assumption is applied to all the other fiscal forecasts we use.

[27] Since these forecasts were constructed prior to 2020, they do not include PEPP purchases; but forecast vintages from 2015 onwards include anticipated purchases under the ECB's earlier asset purchase programme, the APP.

[28] Hence the weighted average maturity of debt in our simulations, in the ELB period and at the time of the PEPP announcement, is five years. This is somewhat lower than the values observed for German and Italian debt during the ELB period (6.5 years and 7.1 years, respectively).

[29] We do not have access to previous vintages of deficit forecasts from the ELB period. Therefore,

tion, we use the annual discount rate $\hat{r} + \phi = 0.5$. This discount rate is the sum of the government's subjective discount rate, and the rate at which rollover crises come to an end; we do not attempt to identify these two components separately.[30] Then, using our projections for primary deficits and net bond redemptions and integrating using (36), we can calculate the anticipated fiscal pressure $\{F_{t+s}\}_{s\geq 0}$ facing Italy at each time t in the ELB period, at each horizon s. Averaging across forecast vintages t, we obtain an average sequence of anticipated fiscal pressure $\{F_{elb}(s)\}_{s\geq 0}$ for each forecast horizon s. On average over the ELB period, fiscal pressure was expected to increase over the forecast horizon; hence we find that $F_{elb}(s)$ is increasing with s, which will be important for our results since it implies that the sovereign spread increases with maturity. We will write the average fiscal pressure actually experienced by Italy over the ELB period (i.e. the average at horizon $s = 0$) as $F_{elb} \equiv F_{elb}(0)$.

Preferred-habitat investors. Finally, to calculate pre-pandemic yields we also need to know the fraction of net debt held by preferred-habitat investors (as opposed to arbitrageurs) in the pre-pandemic period. Eser et al. (2019), Table 1, report that the fraction of net debt of the big-four euro area economies held by non-Eurosystem preferred-habitat investors was 41.4% in 2014, and 47.0% in 2018. We calibrate the intercept terms in the preferred-habitat equations by taking the average of these two figures, that is, 44.2% of each country's ELB period net debt. Together with the simplifying assumption that bond supply was uniform across maturities over this period, these data nail down the intercept terms $h_{elb}(\tau)$ and $h^*_{elb}(\tau)$ in the preferred-habitat demand equations.

Calibrating risk aversion. Turning now to the degree of risk aversion γ, note that the Core term premium $y^{TP*}(\tau)$ is zero at $\gamma = 0$, and increases with γ. Hence, after subtracting the expectations component implied by the calibrated short rate process out of the yield curve, the German term premium offers us a natural target for identifying γ. Considering an initial risk-free rate $r_t = r_{elb} = -49$bp, and given the average anticipated debt market dynamics from the ELB period described above, we find that setting $\gamma = 0.103$ best fits the German 10-year yield from 2013-2019. The fit is illustrated in the left panel of Figure 2, which shows the model-generated German yield curve (solid

to evaluate the anticipated deficits d_{t+s} in equation (36), we use actual realizations of deficits up to 2019, and 2019-vintage forecasts thereafter.

[30] Similar results are obtained if we instead double or halve the discount rate, setting $\hat{r} + \phi = 1$ or 0.25. These results are available upon request.

Figure 2: Decomposing model-generated yield curves: Germany and Italy

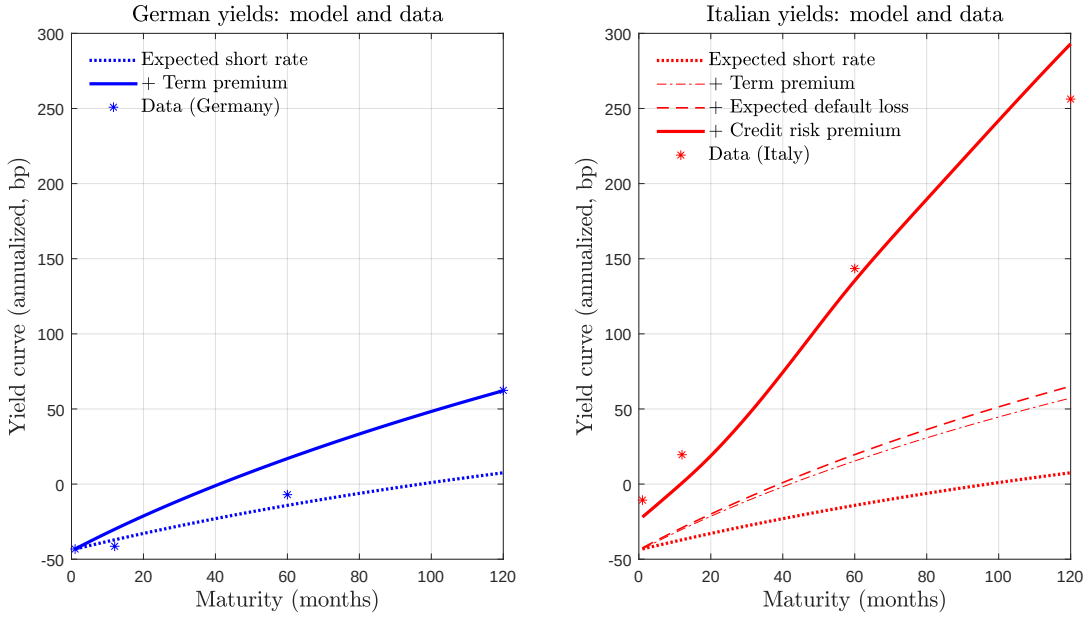

Notes. Sources: Datastream and model simulations.

Left panel. *Stars*: average yields (annualized, basis points) on zero-coupon 1m, 1Y, 5Y and 10Y German sovereign bonds, 2013-2019.

Blue lines: Decomposition of model-generated pre-pandemic German yield curve $y^*_{elb}(\tau)$ into expectations component (dotted) plus term premium (solid).

Right panel. *Stars*: average yields (annualized, basis points) on zero-coupon 1m, 1Y, 5Y and 10Y Italian sovereign bonds, 2013-2019.

Red lines: Decomposition of model-generated pre-pandemic Italian yield curve $y_{elb}(\tau)$ into expectations component (dotted), plus term premium (dash-dotted), plus expected default loss (dashed), and plus credit risk premium (solid).

line) for the ELB period. The expectations component $y^{EX*}_{elb}(\tau)$ is shown as a dotted line; it is increasing because the low risk-free rate of the ELB period is expected to converge back to its long-run value, $\bar{r} = 1\%$. The difference between the dotted and solid lines is the term premium component $y^{TP*}_{elb}(\tau)$.[31] The stars show mean German yields, 2013-2019, for 1m, 1Y, 5Y and 10Y maturities.

Calibrating the default probability. Next, conditional on γ, we estimate the default probability function by matching Italian yields from the ELB period, and their

[31] The resulting average German 10-year term premium over the ELB period is slightly above 50 bp. This is in the ballpark of empirical estimates for this time period (see e.g. Fig. 1 of Lemke and Werner, 2020).

response to the PEPP announcement. Of course, yields are also affected by the default haircut δ; we set $\delta = 0.25$ in light of international evidence.[32] To calibrate the probability function, we assume that the distribution of the default cost, $\Phi(\chi)$, is uniform over an interval $[\underline{F}, \overline{F}]$ sufficiently wide to include all the fiscal scenarios we consider. Then, using $\psi_t = \eta\Phi(F_t + const.)$, the default probability can be written as

$$\psi_t = \psi_{elb} + \theta\left(F_t - F_{elb}\right). \tag{37}$$

where $\theta \equiv \eta/(\overline{F} - \underline{F})$ equals the arrival rate η of a rollover crisis times the density $1/(\overline{F} - \underline{F})$ of the uniform distribution Φ, and ψ_{elb} is an intercept term associated with the average fiscal pressure experienced in the ELB period.[33]

Minimizing the distance from the model's predictions to the Italian yield curve in the pre-pandemic ELB period (2013-2019) and to the shift in the curve induced by the PEPP announcement (discussed in the next section) we estimate $\psi_{elb} = 3$bp *per annum*, and $\theta = 4.03\times10^{-5}$, respectively.[34] Thus, the expected instantaneous default loss, $\delta\psi_{elb}$, evaluated at the mean fiscal pressure F_{elb} actually experienced during the ELB period, was very small, less than one basis point annually. However, fiscal conditions were not expected to be constant over this period. Instead, fiscal pressure was expected, on average, to increase over the forecast horizon ($F_{elb}(s)$ increases with s), implying a rising default probability over time, reaching $\psi_{t+s} = 57$bp at a horizon of ten years. Even so, this still implied a very small expected default loss $y^{DL}_{elb}(\tau)$, seen as the distance between the dash-dot and dashed lines in the right panel of Figure 2. The much larger component of the sovereign spread is the credit risk premium $y^{CR}_{elb}(\tau)$, which is the distance between the dashed and solid lines in the figure. Note that the two premia, $y^{DL}_{elb}(\tau)$ and $y^{CR}_{elb}(\tau)$, are both increasing with maturity τ, because of the anticipated trend in fiscal pressure and the default probability. Together, the two components are consistent with the level and term structure of the Italian sovereign premium (the red stars in the figure show Italian yields, 2013-2019).[35]

[32] Cruces and Trebesch (2013) find haircuts on the order of 50% in evidence drawn mostly from emerging markets; for advanced economies we feel that a smaller haircut is more plausible.

[33] The uniformity assumption implies that the slope θ inferred by matching the impact of the PEPP announcement can also be used to infer the impact of the alternative policies analyzed in Sec. 5.

[34] We estimate the response of the default probability to fiscal pressure, θ, without attempting to identify the arrival rate of a rollover crisis, η, separately from the derivative $\Phi' = 1/(\overline{F} - \underline{F})$.

[35] In the alternative calibration strategy discussed in the appendix, where we treat the ELB period

4.2 Dynamics: the PEPP announcement, the pandemic, and the yield curve

The slope parameter θ that links fiscal pressure with the default probability is also crucial for matching the shifts in peripheral yields observed over the course of the pandemic. Strikingly, the yield curve impact of the PEPP announcement looks almost like a mirror image of the preceding shifts caused by the pandemic, as Figure 1 showed. As the pandemic began to spread, the Spanish and Italian yield curves shifted up in a roughly parallel fashion, with a modest downwards shift and steepening in German yields (the left panel of the figure compares average yields over the week of Feb 13-19 with yields one month later, over the week of 12-18 March, just before the PEPP announcement). Much of this rise was reversed, by roughly parallel downward shifts in Spanish and Italian yields, upon the announcement of PEPP (the right panel compares end-of-day yield curves for March 18 and 20, before and after the announcement).

Expectations before and after the PEPP announcement. As the pandemic took hold in Italy, Spain, and the rest of Europe, it became clear that a massive fiscal response would be needed, implying higher expected gross debt levels. But shortly thereafter, the PEPP announcement revealed that much of this new debt would be taken onto the Eurosystem's balance sheet. In standard (no default) models of risk-averse arbitrageurs, these changes in net supply would steepen the yield curves as the pandemic spread, and flatten them when PEPP was announced, *via* changes in term premia. But in our model, the impact of purchases on yields is reinforced by several additional effects related to default. On one hand, a reduction in the net supply of defaultable bonds $S_t(\tau)$ shrinks the credit risk premium $y_t^{CR}(\tau)$ that markets demand to hold those bonds. This effect operates even when the default probability is exogenous. On the other hand, with endogenous default, lower net bond supply decreases future net redemptions $S_{t+s}(0)$ and hence reduces the default probability (both at t and at future times $t+s$). This lowers the expected default loss $y_t^{DL}(\tau)$ and also reinforces the fall in the credit risk premium (see eqs. 18 and 23).

To evaluate the impact of the PEPP announcement, we use the ECB/Eurosystem projections of German and Italian gross debt around that announcement. For an initial time t that corresponds to March, 2020, we simulate a no-PEPP scenario,

as if it were a steady state, the components $y_{elb}^{DL}(\tau)$ and $y_{elb}^{CR}(\tau)$ are instead constant across maturities. This is counterfactual, since it makes the sovereign spread approximately independent of maturity.

$\{f^{CB}_{t+s}(\tau), f^{CB*}_{t+s}(\tau)\}^{before}_{\tau\geq 0, s\geq 0}$, in which ECB bond holdings are determined by the earlier Asset Purchase Programme (including the expansion of APP on March 12, 2020), and a scenario $\{f^{CB}_{t+s}(\tau), f^{CB*}_{t+s}(\tau)\}^{after}_{\tau\geq 0, s\geq 0}$, in which the APP is complemented by PEPP purchases, as announced on March 18, 2020. We interpret the difference between the two scenarios as the effect of the PEPP announcement. Both scenarios assume the same sequences $\{d_{t+s,} f_{t+s}(\tau), f^{*}_{t+s}(\tau)\}_{\tau\geq 0, s\geq 0}$ of deficits and gross bond supply, which are averages of fiscal forecasts from March and June, 2020.[36] With these data in hand, we can calculate the effects on the term premium and the credit risk premium that go directly through the net stock of bonds, as well as the effects on the credit risk premium that go through fiscal pressure and the default probability via equations (36)-(37).

We focus on the immediate effects of PEPP as it was originally announced in March, with an overall envelope of 750 billion euros to be spent over the course of 2020; these effects capture well the actual causal impact of the announcement, given its unexpected nature.[37] Since the path of purchases under PEPP was flexible, rather than pre-defined like the APP, we must make some assumptions regarding arbitrageurs' expectations about the eventual use of PEPP's flexibility at the time of the March announcement. Our baseline scenario assumes that arbitrageurs anticipated PEPP purchases through June 2020 with perfect foresight – implying some frontloading, and some excess purchases of Italian debt, compared with Italy's capital key (the upper left panel of Figure 7 graphs purchases in this scenario). We assume that from July to December, PEPP purchases were expected to accrue at a constant pace, up to the original PEPP envelope, while maintaining the deviations from capital key that were observed through June.[38] We then estimate the parameter θ to fit the shift in the Italian yield curve when expectations are revised, following the March 18 announcement, from the no-PEPP scenario

[36] To adequately capture expectations of future deficits and net bond supply in the early, pre-PEPP weeks of the pandemic crisis, we average across fiscal forecasts in the March and June, 2020, ECB/Eurosystem projections. Due to the closing date for the March 2020 projections, these still did not include estimates of the full impact of the pandemic on national government debts, so they do not capture investor expectations right before the PEPP announcement. The June projections did include a more updated, realistic estimate, but based partly on information that was not available to investors in mid-March. Thus, the average of the March and June fiscal projections provides a reasonably good proxy of investors expectations immediately ahead of the PEPP announcement.

[37] Subsequent recalibrations of the PEPP purchase envelope (in June and December that year) were largely anticipated by the market, according to different surveys.

[38] Note that our simulation scenarios treat the PEPP envelope as a limit on the total face value of purchases. In reality, it limited the total market value of purchases. Assuming a limit on the face value instead simplifies our calculations, since it allows us to avoid a fixed point loop in the bond price.

Figure 3: Effects of PEPP announcement: baseline scenario.

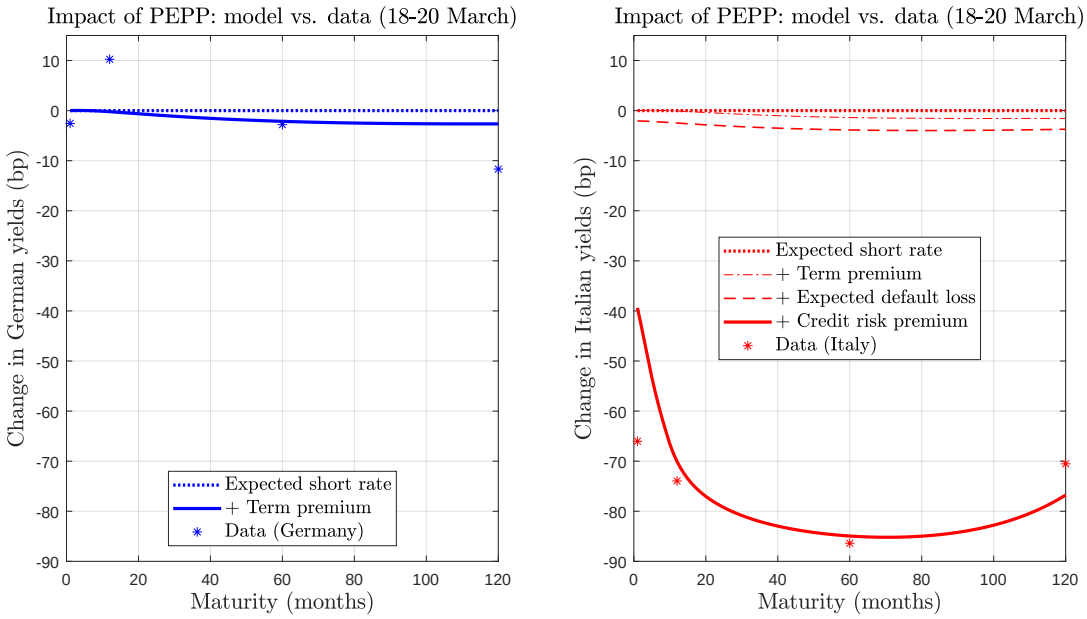

Notes. Sources: Datastream and model simulations.

Left panel. Blue stars: shift in German yields, 18 to 20 March 2020.

Blue lines: model decomposition of shift in German yields into expectations component (dotted) plus term premium (solid), in response to purchase announcement seen in top, left panel of Fig. 7.

Right panel. Red stars: shift in Italian yields, 18 to 20 March 2020.

Red lines: model decomposition of shift in Italian yields into expectations component (dotted), plus term premium (dashed-dotted), plus expected default loss (dashed), and plus credit risk premium (solid), in response to purchase announcement seen in top, left panel of Fig. 7.

to the PEPP scenario.

Impact of PEPP announcement. The results under the estimated value of θ are shown in Figure 3, where stars indicate the change in yields between March 18 (pre-announcement) and March 20, 2020 (after the PEPP announcement).[39] The blue stars in the left panel show that the PEPP announcement had a small, nonmonotonic impact on German yields, which rose at a one-year maturity and fell at five- and especially ten-year maturities. In contrast, the impact on Italian yields was dramatic (right panel, red stars), showing a hump-shaped decline that had its largest impact, of almost 90

[39] We take the change from March 18 to 20 as our measure of the impact of the PEPP announcement, because yields were still volatile across Europe on the 19th, but settled down from the 20th onwards.

basis points, at a five-year maturity. Hence, across all maturities, the announcement was associated with a large reduction in average eurozone bond yields, together with a sharp drop in cross-country differentials.

Our model does a good job of reproducing the effect on yields in both countries. Given the degree of risk aversion implied by our calibration, the PEPP announcement is predicted to cause a modest decline in the German term premium, of roughly three basis points.[40] The effect on the Italian term premium is similar. This is to be expected in the light of Proposition 2, which says that term premia are approximately equalized in a monetary union if the default probability is low. However, the sovereign spread on Italian debt declines sharply, first of all because the increased absorption of credit risk makes the market much more willing to take part of this risk into its own hands. Moreover, under our estimated parameters, the PEPP announcement caused a small decline in the expected default costs on Italian debt, on the order of three basis points *per annum*, seen as the difference between the dashed and dash-dot lines in the right panel of Fig. 3. While this change is small in absolute terms, it represents a nontrivial reduction in the already small level of the expected default loss on Italian debt. Concretely, the model-implied expected default loss hovered between 12 and 14 basis points *per annum* over the initial months of the pandemic in the absence of PEPP, so the announcement appears to have reduced the default probability by almost one quarter. Therefore, the model suggests that the extraction of defaultable bonds from the market, together with the resulting reduction in their default risk, jointly caused a large decrease in the credit risk premium $y_t^{CR}(\tau)$, which accounts for the largest share of the response to the PEPP announcement.

The reduction in Italian yields at the time of the announcement is large at all maturities, but is strongest for bonds of intermediate duration, which will be maturing when cumulative net purchases are still large. In contrast, one-month bonds mature before many purchases have taken place. At the opposite extreme, for ten-year bonds, our scenario implies that most net redemptions will have occurred, and hence yields will be rising again, by the time the bonds mature. Since yields are forward-looking, the future return to normality limits the change in 10-year yields on impact.

Beyond its powerful effect upon announcement, our model also implies that PEPP has a persistent effect on yields over time. Figure 4 illustrates the impulse responses

[40] Since the model treats the riskless short rate as an exogenous factor, changing the path of purchases has no impact on the expectations component $y_t^{EX}(\tau)$.

Figure 4: Persistence of PEPP effects: baseline scenario.

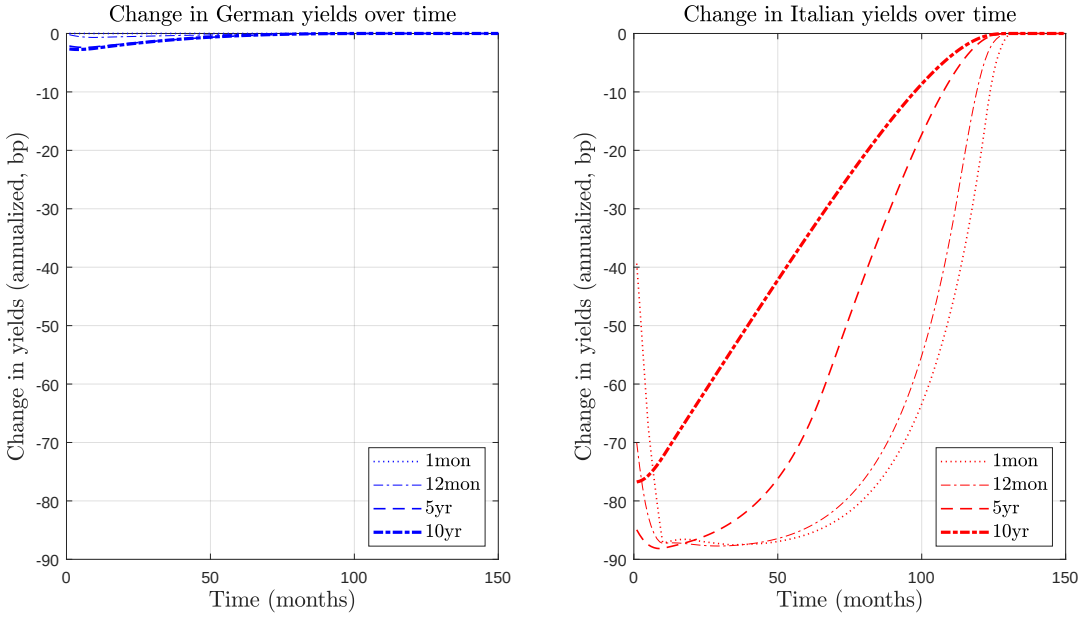

Notes.
Left panel. PEPP effects on German yields over time, for one month, one year, five year, and ten year maturities, under the baseline purchase program seen in top, left panel of Fig. 7.
Right panel. PEPP effects on Italian yields over time, for one month, one year, five year, and ten year maturities, under the baseline purchase program seen in top, left panel of Fig. 7.

of yields to the PEPP announcement, for one-month, 12-month, 60-month, and 120-month maturities, under the assumption that the purchase program unfolds as expected under our baseline scenario. The small decrease in German yields (left panel) mostly affects long bonds, and decays smoothly, with a half-life of roughly three years. The much larger reduction in Italian yields (right panel) is very persistent, but differs across durations. The impact on 10-year bonds declines smoothly over time, while for one-month and one-year bonds the effect is initially increasing, building up to a reduction in yields of roughly 90 basis points in the second year after the announcement.

To understand how these responses vary with duration, note that our simulations assume that gross public issuance and gross ECB purchases are both uniform across maturities, and that purchases are held to maturity. The effect on short yields increases over the course of 2020, because the quantity of short bonds held increases over that period, accumulating new purchases with bonds purchased earlier at slightly greater maturity. The trough in short yields occurs just as gross purchases cease. From this

Figure 5: Impact of PEPP on sovereign premium and CDS spreads

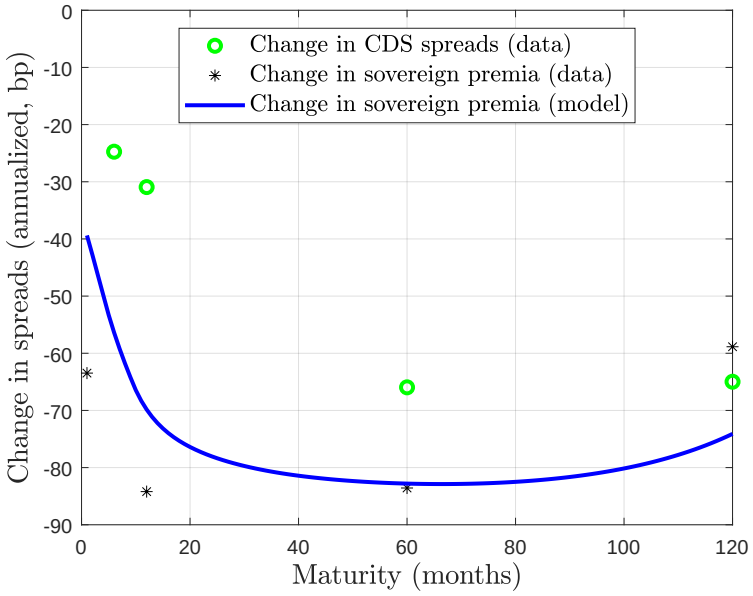

Notes. Sources: Datastream and model simulations.
Effects of the PEPP announcement on the sovereign premium and CDS spreads (March 18-20, 2020). Black stars show the change in the sovereign premium on Italian over German debt (1 month, 12 month, 5 year, and 10 year maturities). Green circles show the change in the Italian CDS spread (6 month, 12 month, 5 year, and 10 year maturities). The solid blue line shows the model-generated change in the sovereign premium.

time onwards, the whole portfolio gradually matures; the decrease in 10-year yields from 2021 onwards (i.e. after the end of the net purchase phase envisioned in the original PEPP announcement) is only due to arbitrage across durations, not because the program still holds any bonds with a 10-year residual maturity. As the average maturity of the PEPP portfolio shortens, its impact on long yields fades away, followed by its impact on short yields. The final effects of the program disappear as the last bonds mature, 120 months after the end of gross purchases.

CDS spreads. To further validate the performance of our model, we can also examine the effect of the PEPP announcement on credit default swap (CDS) spreads, shown by the green circles in Figure 5. When a default (or related credit event) occurs, a CDS pays off the difference between the face value of the defaulted bond and its

remaining market value. Hence the payoff to a CDS is equal to that of a portfolio that is long one default-free bond and short one defaultable bond. Ignoring transactions costs and assuming absence of arbitrage, this implies that the per-period price of holding a CDS (the spread that is paid as a premium on the CDS contract) must equal the price of holding such a portfolio (Duffie, 1999) which in our case is simply the sovereign spread, that is, the yield on an Italian bond minus the yield on a German bond of the same maturity. Hence, abstracting from transactions costs and arbitrage opportunities, upon the announcement of PEPP, CDS spreads and the Italian-German sovereign spread should fall by the same amount. This prediction is close to being true at 5-year and especially 10-year maturities, but fails at short maturities, where the observed decrease in the CDS spread is substantially smaller than the observed decline in the sovereign premium. Interestingly, our model's prediction for the impact of PEPP lies mostly between the observed impacts on CDS spreads and sovereign spreads.

Impact of the pandemic outbreak. As an additional quantitative cross-check on our model, we can study how the pandemic itself affected German and Italian yields. In this context, we view the economic impact of the pandemic as a large, unexpected increase in deficits and public debt issuance over the medium term. To quantify this change in fiscal expectations, we take December 2019 ECB/Eurosystem fiscal projections for Germany and Italy as a proxy for expectations in the absence of the pandemic, and we take the average of the corresponding March 2020 and June 2020 forecasts as a proxy for expectations that include the pandemic and the associated pre–PEPP policy responses.[41] Figure 6 shows the model-generated shift in yield curves associated with this change in expectations. The model response is compared to the observed shift in yields from the week of 13-19 February, 2020, when the pandemic was not yet expected to have a major impact, to the week of 12-18 March, when peripheral yields were spiking in response to the pandemic but the PEPP had not yet been announced.

Beyond the change in fiscal expectations related to the pandemic, there was also a decrease in German short-term rates between February and March 2020, which our simulations treat as a shock to r_t. Together, the revised fiscal expectations and the

[41] The ECB's expansion of the Asset Purchase Programme envelope by 120 billion euros on March 12, 2020 is accounted for in the updated March-June fiscal expectations. As explained before, the average of the March and June fiscal projections provides a reasonable proxy of investors' expectations in the first few weeks of the pandemic crisis, before the original PEPP announcement.

Figure 6: Impact of the pandemic outbreak

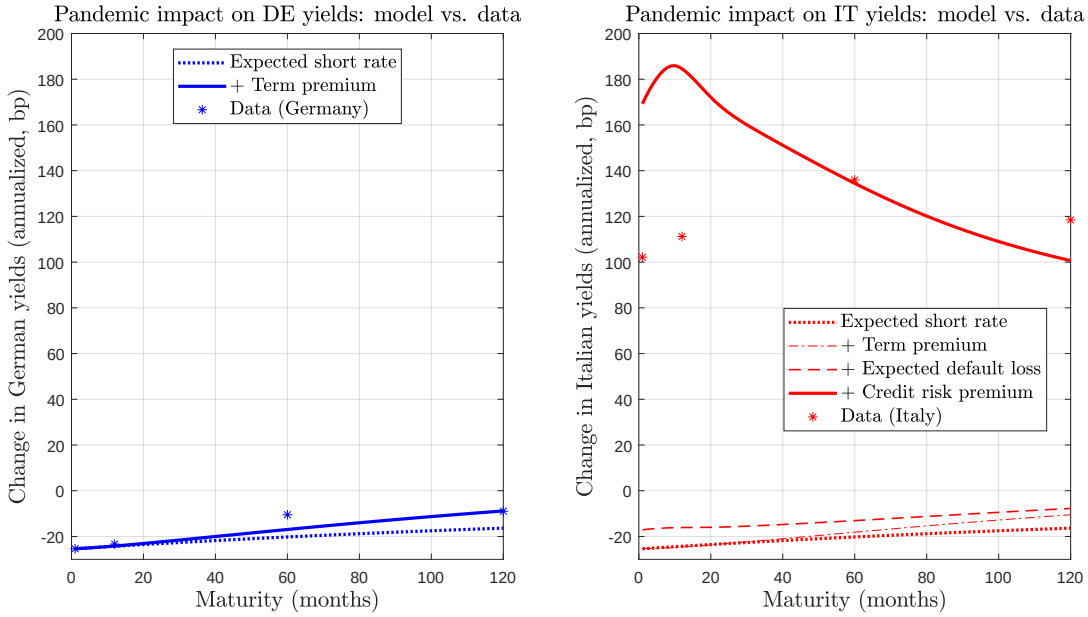

Notes. Sources: Datastream and model simulations.

Left panel. Blue stars: shift in weekly average German yields from week of 13-19 February 2020 to week of 12-18 March 2020.

Blue lines: model decomposition of shift in German yields into expectations component (dotted) plus term premium (solid), in response to revised fiscal expectations associated with the pandemic.

Right panel. Red stars: shift in weekly average Italian yields from week of 13-19 February 2020 to week of 12-18 March 2020.

Red lines: model decomposition of shift in Italian yields into expectations component (dotted), plus term premium (dashed-dotted), plus expected default loss (dashed), plus credit risk premium (solid), in response to revised fiscal expectations associated with the pandemic.

shock to the riskless rate explain the downward shift and steepening of the German yield curve shown in the left panel of Fig. 6. The downward shock to the riskless rate causes the expectations component $y_t^{EX*}(\tau)$ to become steeper, while the change in fiscal expectations steepens the term premium $y_t^{TP*}(\tau)$ by a similar amount; together, these two effects are quantitatively consistent with the observed change in the slope of the German yield curve (blue stars in the figure). The right panel of the figure shows that the change in fiscal expectations associated with the pandemic generates a large upward shift in Italian yields in our model (red curves), of the same order of magnitude as the shift observed in bond markets from February to March 2020 (red stars). The model

overpredicts somewhat the market reaction at short maturities, and underpredicts it for ten-year bonds, but for five-year yields the model-generated change is very close to that in the data, rising by approximately 140bp. Most importantly, our model is consistent with the upward shift observed in the Italian yield curve, a feature that cannot be explained by a standard model without default. Thus, applying our model to the initial pandemic shock appears to validate the calibration that best matches the impact of PEPP. In both contexts, our model of endogenous default probabilities allows us to generate large shifts in yields across all maturities, driven by the credit risk premium component $y_t^{CR}(\tau)$, in contrast with the impact that would be observed if duration extraction were the only relevant transmission channel.

5 Counterfactual policy experiments: flexibility and effectiveness of purchases

Since our assumption that the peripheral default probability varies with the degree of fiscal pressure appears to match the impact of PEPP well, across jurisdictions and maturities, we now apply our model to evaluating counterfactual policy scenarios. In particular, we are interested in evaluating how the flexible design of the PEPP purchases altered their impact, relative to the design of earlier ECB programs. Figure 7 illustrates four of the policy scenarios we will consider.

The top, left panel shows the baseline scenario that we used in Section 4.2 as a stand-in for expectations regarding the PEPP upon its announcement. The blue line shows our scenario for cumulative PEPP purchases of German sovereign bonds (expressed in face value, in billions of euros) for months 3-12 (indicating March-December, 2020). Likewise, the red line shows our scenario for Italian purchases. The path of purchases up to the end of June represents actual PEPP purchases, which accumulated almost linearly over time, at a pace that, if continued, would have exhausted the envelope before the end of the year. As a fraction of the monthly total, Italian purchases exceeded Italy's capital key, while purchases of German bonds were close to capital key (purchases of French bonds were substantially below capital key). Since our scenario is intended to model the effects of the initial announcement, we abstract from the actual path of purchases after June (when a recalibration of the PEPP purchase envelope was announced), and instead suppose that purchases from July onwards would use up the

Figure 7: Baseline purchase scenario and counterfactual experiments.

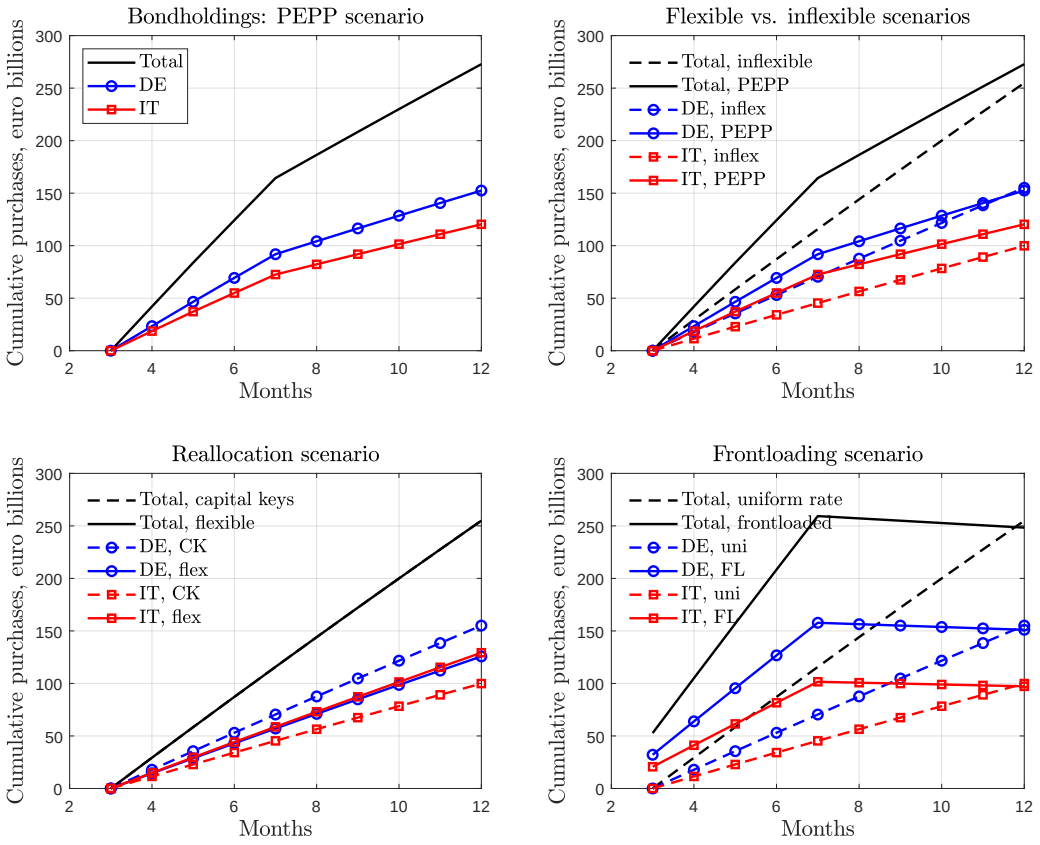

Notes.

Top, left panel: Baseline model scenario for PEPP purchase expectations as of March 2020. Blue circles: Germany; red squares: Italy; black: aggregate face value. Effect on yields is shown in Figs. 3-4.

Top, right panel: Comparing baseline PEPP scenario vs. inflexible "APP-style" scenario with a constant pace of purchases and allocations equal to capital keys. Blue circles: Germany; red squares: Italy; black: aggregate face value. Effect on yields is shown in Fig. 8.

Bottom, left panel: Comparing inflexible "APP-style" scenario with a scenario that reallocates purchases by ±5%. Blue circles: Germany; red squares: Italy; black: aggregate face value. Effect on yields shown as a black dash-dot line in the left panel of Fig. 9.

Bottom, right panel: Comparing inflexible "APP-style" scenario with a "frontloading" scenario that completes all purchases by July. Blue circles: Germany; red squares: Italy; black: aggregate face value. Effect on yields shown as a green dotted line in the left panel of Fig. 9.

remaining PEPP envelope at a constant pace, while maintaining the initial deviations in capital key. The black line represents cumulative purchases of the whole PEPP program in our two-country model – that is, it is the sum of the blue and red lines.

APP-style purchases. We first compare our PEPP scenario to a counterfactual alternative following the inflexible design principles of the earlier Asset Purchase Programme (APP). That program imposed a constant pace of purchases over a pre-specified period of time, and allocated purchases according to each eurozone state's capital key. Building upon these features, we design a hypothetical "APP-style" purchase announcement whereby the ECB would have committed to the same overall envelope, but would have distributed the purchases linearly over time, and according to a strict application of the capital key. This comparison is illustrated in the top, right panel of Fig. 7. There, the blue dashed line represents a constant rate of German bond purchases from March to December that add up to Germany's capital-key share (26.4%) of the PEPP envelope.[42] Likewise, the red dashed line represents purchases of Italian bonds, at a constant rate, that add up to Italy's capital-key share (17.0%) of the PEPP envelope. The black dashed line represents total cumulative purchases under our "APP-style" counterfactual, so it is the sum of the blue and red dashed lines. As before, the blue, red, and black solid lines represent cumulative purchases under our benchmark flexible PEPP scenario (German, Italian, and total bonds, respectively). Clearly, our PEPP scenario imposes frontloading, with an initial pace of purchases faster than the APP design would permit. Simultaneously, our PEPP scenario allocates more purchases to Italy than the APP design would, while total purchases of German debt in our PEPP scenario are similar to those in our APP scenario (close to capital key). Hence total PEPP purchases (black solid line) end up slightly above the intended envelope (black dashed line) since our two-country simulation abstracts from the jurisdictions where purchases were lowest, relative to capital key.

Figure 8 shows how the effects of the purchase program differ between the PEPP and APP designs. The figure shows the yields resulting from the PEPP scenario minus those under the APP scenario, so the fact that the differences shown in the graphs are negative indicates that the PEPP design reduces yields more than the APP design does. The top row (like Fig. 3) decomposes the effects on the yield curve at the time of the announcement; the left column refers to Germany, while the right column refers to

[42] While the total PEPP envelope was 750 billion euros, we only analyze the part that was dedicated to sovereign bonds (608 billion), abstracting from private-sector and supranational purchases.

Figure 8: Comparing impact of PEPP scenario with "inflexible" alternative

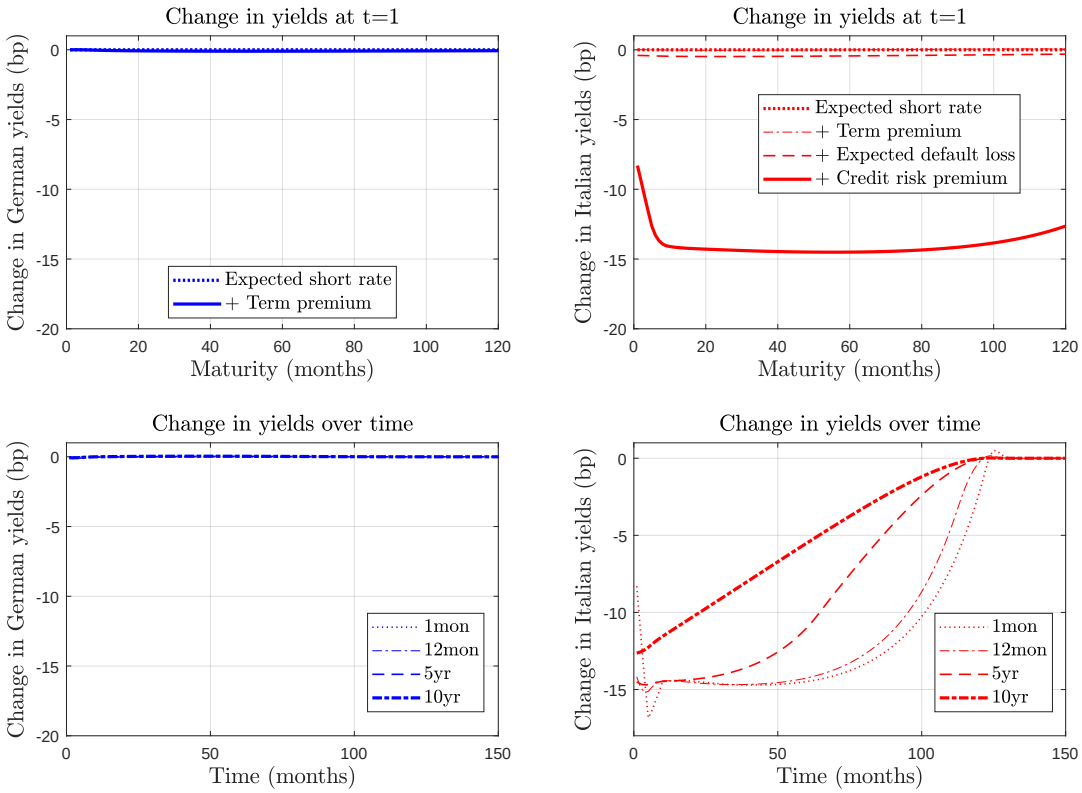

Notes.

Panels show the difference between the baseline PEPP scenario and an "APP-style" scenario that imposes a constant pace of purchases and allocations equal to capital keys, as illustrated in top, right panel of Fig. 7.

Italy. The PEPP design causes a small extra reduction in German yields, by half a basis point at longer maturities, compared to the APP-style program. But the reduction in yields is much more significant in the Italian case, where PEPP shifts the yield curve by almost fifteen additional basis points at most maturities, compared with the APP design. Most of the difference between the PEPP and APP designs is attributable to a decline in the credit risk premium (the distance between the dashed and solid red lines in the top, right panel of the figure). In the bottom row (as in Fig. 4), we see that the additional impact of the flexible PEPP design is persistent. The impact of flexibility on ten-year and five-year yields has a half life of about four and six years, respectively.

Effects of flexibility in cross-country allocation and timing. Which aspect of the flexibility of PEPP is most important for its stronger impact on yields, as com-

pared with an APP design? We next perform additional counterfactual experiments to distinguish the role of flexibility in the cross-country allocation of purchases from flexibility in their timing. The black dash-dot line in the left panel of Figure 9 documents the effect of cross-country allocation alone. Taking the APP design as a starting point, it considers the impact of reallocating purchases worth five percentage points of the overall PEPP envelope from Germany to Italy. This change in purchases is illustrated in the bottom, left corner of Fig. 7, which shows an increase in Italian purchases and a decrease in German purchases, with total purchases (black line) unchanged. The impact on Italian yields is striking. Reallocating purchases causes a large, persistent decrease in Italian yields (top panel of Fig. 9) of 16 to 19 basis points across most maturities, which is quite similar to the overall impact of the PEPP design. In contrast, the impact on German yields (not shown) is negligible, as we saw earlier in Fig. 8.

These results again reflect Proposition 2, which showed that when default risk is low, term premia are driven by the overall quantity of purchases, not their distribution across jurisdictions. Since the expectations term is not affected by purchases at all in our model, we can furthermore conclude that if Italian default risk is low, then the German yield curve is determined by the total quantity of purchases, regardless of how those purchases are distributed. But for Italy, country-specific purchases are crucial for yields, because decreasing free-floating default risk makes the market more willing to hold this risk. Again, the actual impact on expected losses from default is tiny – the additional purchases of Italian debt decrease the expected losses from Italian default by less than one basis point (the "DL" component). But when part of this risk is taken off the market, arbitrageurs become much more willing to bear the remaining risk, lowering the credit risk premium by almost 20bp at intermediate maturities (the "CR" component). Hence, from the point of view of reducing average euro area yields, reallocating purchases from Germany to Italy makes the purchase program much more effective. In other words, flexibility in allocation across countries is an important factor in explaining the effectiveness of the PEPP design.

The green dotted line in the left panel of Figure 9 instead isolates the impact of flexibility in timing. It considers a frontloading scenario in which all purchases are realized in the first five months of the purchase program, as compared with the APP scenario in which the pace of purchases is constant through December 2020 (these two possible purchase paths are compared in the bottom, right panel of Fig. 7). This comparison relates to timing only, so it does not contemplate any deviation from capital

Figure 9: Effects of flexibility in cross-country allocation and timing

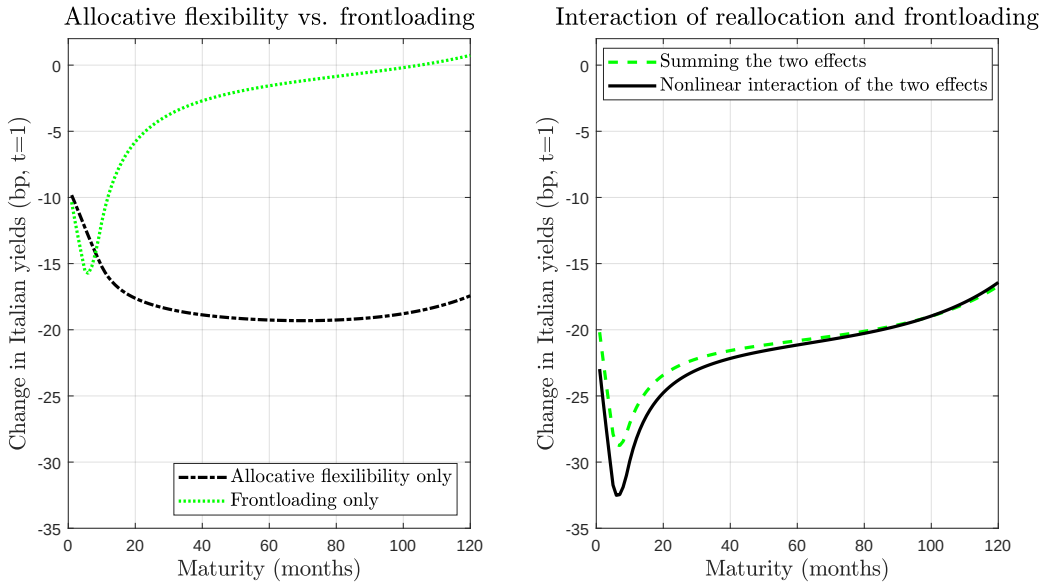

Notes.
Comparing the impacts on Italian yields of reallocation of purchases across countries, and frontloading over time, separately and jointly.
Left panel. The black dash-dot line shows the effect of reallocating 5% of the total PEPP envelope from Germany to Italy; the green dotted line shows the effect of frontloading all PEPP purchases into the first five months, instead of maintaining a constant purchase pace from March to December.
Right panel. The green dashed line shows the sum of the two effects from the left panel. The black solid line shows the combined impact of implementing the reallocation and frontloading policies together.

keys; but note that the frontloading in this exercise is substantially stronger than the frontloading in our baseline PEPP scenario. This frontloading causes a tiny decrease, on impact, in the German yield curve (not shown). For Italy (left panel of Fig. 9) it causes a large decrease in short yields on impact, of more than 15bp for six-month maturities, but at the same time, it causes a tiny increase in ten-year yields. Frontloading implies an increase in the flow of purchases early in the program, but by the same token it implies a decrease in this flow later, and eventually causes the whole portfolio to mature earlier. Hence, the impact of frontloading over time is a sharp decrease in most yields at the beginning of the program, but a small increase later, when the portfolio matures. These future effects are priced into Italian ten-year yields from the very beginning.

We have seen that reallocation can have a big impact on Italian yields, with negligi-

ble effects on German ones, while frontloading trades off a large decrease in short-term Italian yields against a small increase in the longest Italian yields. But how do these policies interact? The right panel of Figure 9 addresses this question by comparing the individual effects of flexibility across jurisdictions, and flexibility over time, to their joint effect. The green dashed line sums the impact of flexibility across jurisdictions only plus the impact of frontloading only (that is, it sums the the two curves from the left panel). The black solid line instead shows the joint, nonlinear effect of a policy that combines reallocation across jurisdictions (redistributing purchases from Germany to Italy, away from their capital keys, as illustrated in the lower, left panel of Fig. 7) with frontloading over time (as illustrated in the lower, right panel of Fig. 7). Hence, the difference between the black solid line and the green dashed line shows that reallocation and frontloading interact in a nonlinear way. In particular, combining reallocation with frontloading decreases short yields by up to 32 basis points, while the impact of the two policies separately sums to only 28 basis points for the same maturities. We conclude that flexibility across jurisdictions and flexibility across time are complements, rather than substitutes: each aspect of flexibility contributes individually to the effectiveness of asset purchases, and more so jointly.

Reinvestments. Finally, we analyze the importance of another design feature that increases the effectiveness of asset purchases, namely, reinvestment of maturing bonds. Without changing the structure of the initial purchases, the impact of the program on yields is increased if maturing bonds are reinvested after net purchases end, thus preserving the central bank's absorption of duration and default risk over a longer horizon. In Figure 10, we consider a variation on our baseline PEPP scenario (which abstracts from reinvestment commitments, consistently with the original PEPP announcement) that includes a commitment to reinvest all maturing bonds in 10-year bonds, for a period of five years, after which the whole portfolio is held to maturity. Note that since our baseline PEPP scenario assumed that purchases would be uniform across maturities, reinvesting in 10-year bonds maintains this uniform distribution across maturities throughout the five-year reinvestment period.

Figure 10 reports the difference in the behavior of yields between the PEPP scenario with reinvestment, and the baseline PEPP scenario we saw earlier. Even though the profile of purchases over the net investment period is unchanged, committing to reinvestment already has a large impact on yields at the time of announcement, especially

Figure 10: Impact of reinvestments

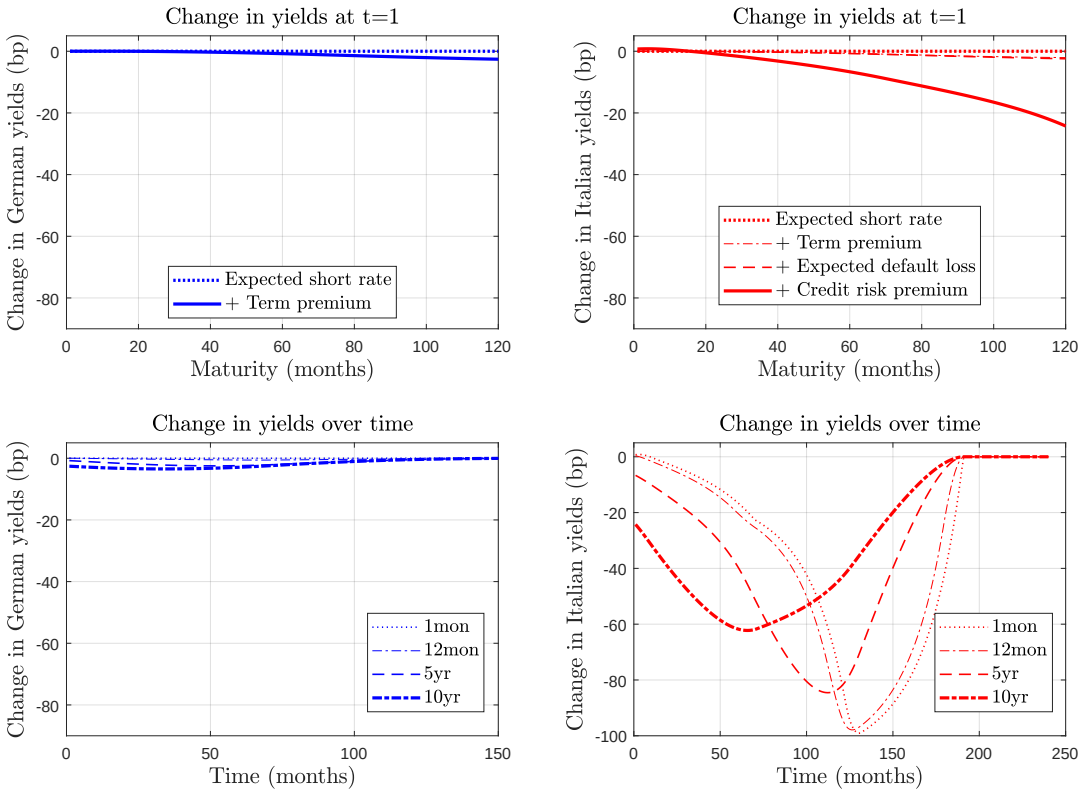

Notes.

Panels show the difference between a scenario in which all maturing bonds are reinvested in new purchases of 10Y bonds, for five years after the end of net purchases, and the baseline PEPP scenario without reinvestment.

for longer bonds.[43] Upon announcement, the program with reinvestment decreases the yield on German 10-year bonds by an additional two basis points, and that on Italian 10-year bonds by an additional 23 basis points. As before, the impact on Italian bonds goes mainly through the credit risk premium, since the reinvestment program decreases for several years the net supply of defaultable bonds that private agents must hold. The decrease in German and Italian yields is persistent, and actually increasing for some time, with the maximum impact on 10-year Italian bonds after five years, and that on Italian short-term bonds (almost 100 basis points) more than ten years down the line. Note that currently the PEPP and APP programs both incorporate reinvestment

[43]For comparability with our earlier exercises, we assume that the whole time path of each scenario is known at the time of the initial PEPP announcement, *i.e.* March 2020.

commitments.[44] Our results suggest that these commitments may significantly boost the effectiveness of these programs at lowering sovereign bond yields.

6 Conclusions

In this paper, we propose a micro-founded model of the term structure of sovereign interest rates in a heterogeneous monetary union. We extend the Vayanos and Vila (2020) affine term structure model to a two-country monetary union in which one of the two sovereign issuers (Periphery) faces default risk, due to the possibility of rollover crises. In addition to the standard and well-documented *duration risk extraction channel* of asset purchase programs, our model features a *default risk extraction channel*, whereby announcements of central bank asset purchases reduce both the expected amount of defaultable bonds to be absorbed by the market and the sovereign default probability itself, thus reducing the compensation risk-averse investors require to absorb default risk.

We apply our model to analyze the impact of the ECB's pandemic emergency purchase programme (PEPP), announced in March 2020 in a context of rising expected issuance of euro area sovereign debt as a consequence of the Covid-19 crisis. We calibrate the model to data on German and Italian yields, by targeting the average shape of both countries' sovereign yield curves in the pre-pandemic period and the change in Italian yields over the two days following the PEPP announcement. Under the inferred parameters, the sovereign credit risk premium is an order of magnitude larger than the expected loss due to default. We show analytically that under this parameter configuration, the term premium and hence German yields depend approximately on aggregate asset purchases, regardless of their cross-country distribution. In contrast, the Italian yield curve depends strongly on how asset purchases are allocated across countries. Quantitatively, we conclude that default risk extraction is the most significant channel to explain the response of the Italian yield curve to the PEPP announcement, much more so than duration extraction.

We then perform counterfactual simulations to evaluate how important the PEPP's flexible design was for its impact. A key feature of the PEPP was flexibility in the

[44] The March 2020 PEPP announcement did not commit to reinvestments, which is why there is no reinvestment under our benchmark scenario. A reinvestment commitment was first announced for PEPP at the end of June, 2020, and remains in place at the time of this writing.

distribution of purchases over time and across jurisdictions. We find that the flexible allocation of purchases permitted by the PEPP design substantially enhanced its impact. The PEPP announcement reduced Italian yields by around 80bp across the yield curve, of which almost 15bp can be attributed to the flexibility of PEPP, as compared with a hypothetical announcement with the same overall envelope but an APP-style design (a constant pace of purchases, allocated across countries according to the ECB's capital key). Overall, since the impact of asset purchase redistributions on German yields is negligible, average euro-area yields depend strongly on the cross-country allocation of purchases, through their effect on peripheral yields.

References

Aguiar, M., M. Amador, E. Farhi, and G. Gopinath (2015). Coordination and crisis in monetary unions. *Quarterly Journal of Economics 130*(4), 1727–1779. 3

Altavilla, C., G. Carboni, and R. Motto (2021). Asset purchase programs and financial markets: Lessons from the euro area. *International Journal of Central Banking 17*, 1–48. 1

Ang, A. and M. Piazzesi (2003). A no-arbitrage vector autoregression of term structure dynamics with macroeconomic and latent variables. *Journal of Monetary Economics 50*, 745–787. 1

Arellano, C., Y. Bai, and G. P. Mihalache (2020). Monetary policy and sovereign risk in emerging economies (NK-default). NBER Working Paper 26671. 3

Arellano, C., X. Mateos-Planas, and V. Ríos-Rull (2019). Partial default. NBER Working Paper 26076. 7, 3

Bacchetta, P., E. Perazzi, and E. van Wincoop (2018). Self-fulfilling debt crises: Can monetary policy really help? *Journal of International Economics 110*, 119–134. 3

Bianchi, J. and J. Mondragon (2018). Monetary independence and rollover crises. Working paper 755, Federal Reserve Bank of Minneapolis. 3

Borgy, V., T. Laubach, J.-S. Mésonnier, and J.-P. Renne (2012). Fiscal sustainability, default risk, and euro area sovereign bond spreads. Banque de France DT350. 1

Broeders, D., L. de Haan, and J. W. van den End (2021). How QE changes the nature of sovereign risk. Manuscript, De Nederlandsche Bank. 1

Calvo, G. (1988). Servicing the public debt: The role of expectations. *American Economic Review 78*(4), 647–661. 1, 3, 3

Camous, A. and R. Cooper (2019). "Whatever it takes" is all you need: Monetary policy and debt fragility. *American Economic Journal: Macroeconomics 11*(4), 38–81. 3

Cole, H. L. and T. J. Kehoe (2000). Self-fulfilling debt crises. *Review of Economic Studies 67*(January), 91–116. 1, 3, 3

Corradin, S., N. Grimm, and B. Schwaab (2021). Euro area sovereign bond risk premia during the Covid-19 pandemic. ECB Working Paper 2561. 1

Corsetti, G. and L. Dedola (2016). The mystery of the printing press: Monetary policy and self-fulfilling debt crises. *Journal of the European Economic Assocation 14*(6), 1329–1371. 1, 3, 3

Cruces, J. and C. Trebesch (2013). Sovereign defaults: The price of haircuts. *American Economic Journal: Macroeconomics 5*, 85–117. 32

De Grauwe, P. and Y. Ji (2013). Self-fulfilling crises in the eurozone: An empirical test. *Journal of International Money and Finance 34*, 15–36. 1

Del Negro, M. and C. Sims (2015). When does a central bank's balance sheet require fiscal support? *Journal of Monetary Economics 73*, 1–19. A.1

Duffie, D. (1999). Credit swap valuation. *Financial Analysts Journal 55*(1), 73–87. 4.2

Duffie, D. and R. Kan (1996). A yield-factor model of interest rates. *Mathematical Finance 6*(4), 379–406. 1

Duffie, D. and K. Singleton (1999). Modeling term structures of defaultable bonds. *Review of Financial Studies 12*(4), 687–720. 1, 2, 3

Eser, F., W. Lemke, K. Nyholm, S. Radde, and A. Vladu (2019). Tracing the impact of the ECB's asset purchase programme on the yield curve. ECB Working Paper 2293. 1, 4.1

Gourinchas, P.-O., W. Ray, and D. Vayanos (2020). A preferred-habitat model of term premia and currency risk. Manuscript, London School of Economics. 1, 2

Greenwood, R., S. Hanson, J. Stein, and A. Sunderam (2020). A quantity-driven theory of term premia and exchange rates. Manuscript, Harvard University. 1

Greenwood, R. and D. Vayanos (2014). Bond supply and excess bond returns. *Review of Financial Studies 27*(3), 663–713. 1, 1

Hamilton, J. and J. C. Wu (2012). The effectiveness of alternative monetary policy tools in a zero lower bound environment. *Journal of Money, Credit and Banking 44*(Supplement), 1–46. 1, 1, 48

He, Z., S. Nagel, and Z. Song (2020). Treasury inconvenience yields during the Covid-19 crisis. Manuscript, Univ. of Chicago. 1

King, T. B. (2019). Expectation and duration at the zero lower bound. *Journal of Financial Economics 134*(3), 736–760. 1

Krishnamurthy, A. (2022). Quantitative easing: What have we learned? Seminar presentation, Princeton Univ., 24 March. 1

Krishnamurthy, A., S. Nagel, and A. Vissing-Jorgensen (2018). ECB policies involving government bond purchases: Impact and channels. *Review of Finance 22*(1), 1–44. 1

Lemke, W. and T. Werner (2020). Dissecting long-term Bund yields in the run-up to the ECB's public sector purchase programme. *Journal of Banking and Finance 111*(105682). 31

Li, C. and M. Wei (2013). Term structure modeling with supply factors and the Federal Reserve's large-scale asset purchase programs. *International Journal of Central Banking 9*(1), 375–402. 1

Na, S., S. Schmitt-Grohe, M. Uribe, and V. Yue (2018). The twin Ds: Optimal default and devaluation. *American Economic Review 108*(7), 1773–1819. 3

Nuño, G., S. Hurtado, and C. Thomas (2022). Monetary policy and sovereign debt sustainability. *Journal of the European Economic Association Forthcoming*. 3

Ray, W. (2019). Monetary policy and the limits to arbitrage: Insights from a New Keynesian preferred habitat model. Manuscript, UC Berkeley. 1

Reis, R. (2013). The mystique surrounding the central bank's balance sheet, applied to the european crisis. *American Economic Review 103*(3), 135–140. 3, A.1

Vayanos, D. and J.-L. Vila (2020). A preferred habitat model of the term structure of interest rates. *Econometrica Forthcoming*. 1, 5, 2, 2, 9, 2.1, 12, 2.1, 6

A Appendix: Modelling details

A.1 Central bank accounting

This paper has focused primarily on bond market equilibrium, without spelling out the broader financial or macroeconomic context. In this appendix, we briefly sketch how our model of central bank behavior fits into a wider environment and is consistent with its budget constraint.

Besides the arbitrageurs and preferred-habitat investors, financial market participants include commercial banks that can hold short-term riskless bonds and central bank reserves (indeed, some of the arbitrageurs may be commercial banks). Arbitrage then ensures that the short-term riskless rate equals the interest rate on reserves.

The balance sheet of the common central bank consists of sovereign bonds on the assets side and bank reserves and capital on the liabilities side. We assume that the central bank maintains separate accounts associated with each national government in the monetary union, and determines seignorage transfers in relation to its holdings of each country's bonds. This structure roughly corresponds to the Eurosystem, in which most bonds are held by the national central banks of the countries that issued those bonds, with only a small fraction of holdings subject to "risk sharing" across the national central banks.

Section 3 showed that the government's loss function in case of repayment depends on the seigniorage policy of the central bank during a rollover crisis. We assume that during a crisis, the central bank pays out to the national government the income it receives from redemptions of the government's bonds minus a fixed amount $\bar{\Gamma}$ aimed at protecting the central bank's capital during the crisis. In other words, we assume a seigniorage rule of the form

$$\Gamma_t = f_t^{CB}(0) - \bar{\Gamma}, \tag{38}$$

so that payments from the government to the central bank to redeem maturing bonds are partially transferred back again to the government in the form of seigniorage. Generally speaking, a rule like (38) may not suffice to avoid an increase in reserves liabilities during a crisis. In normal times, the reserves associated with purchases of peripheral bonds follow[45]

$$\dot{D}_t = r_t D_t + \int P_t(\tau)\, \iota_t^{CB}(\tau)\, d\tau + \Gamma_t - f_t^{CB}(0). \tag{39}$$

In a rollover crisis, equation (38) implies

$$\dot{D}_t = r_t D_t + \int P_t(\tau)\, \iota_t^{CB}(\tau)\, d\tau - \bar{\Gamma}. \tag{40}$$

This will lead to an expansion in the volume of reserves when $\bar{\Gamma} < r_t D_t + \int P_t(\tau)\, \iota_t^{CB}(\tau)\, d\tau$.

We can define the national central bank's capital as

$$K_t \equiv \int \tilde{P}_t(\tau)\, f_t^{CB}(\tau)\, d\tau - D_t,$$

where, as in Del Negro and Sims (2015), $\tilde{P}_t(\tau)$ is a "historical" price that changes only when gross purchases are positive ($\iota_t^{CB}(\tau) > 0$). Capital then evolves as follows,

$$\dot{K}_t = \int \left(\frac{\partial \tilde{P}_t(\tau)}{\partial t} f_t^{CB}(\tau) + \tilde{P}_t(\tau) \frac{\partial f_t^{CB}(\tau)}{\partial t} \right) d\tau - \dot{D}_t.$$

[45] In what follows, for ease of exposition we abstract from the implications of Core bond purchases for the evolution of the common central bank's reserves liabilities and capital. However, it is straightforward to generalize the algebra to account for those implications, without affecting any of our arguments.

During a rollover crisis, equation (40) implies

$$\dot{K}_t = \int \left(\frac{\partial \tilde{P}_t(\tau)}{\partial t} f_t^{CB}(\tau) + \tilde{P}_t(\tau) \frac{\partial f_t^{CB}(\tau)}{\partial t} \right) d\tau - r_t D_t - \int P_t(\tau) \iota_t^{CB}(\tau) d\tau + \bar{\Gamma}.$$

Capital can thus decrease during a crisis, potentially falling below zero. This will depend on the maturity structure of the central bank assets, the path of interest payments on reserves, and the constant term $\bar{\Gamma}$. In particular, a sufficiently large capital retention term $\bar{\Gamma}$ can make the probability of a negative capital event arbitrarily small. In any case, as discussed by Del Negro and Sims (2015) and Reis (2013), a central bank can operate with low or even negative capital (within certain limits). Hence the small probability that the central bank could at some time face negative capital is inessential for our analysis.

A.2 Model solution

Since preferred habitat demand is assumed to be an affine function of yield, equations (17) and (18) imply that the risk prices λ_t and ξ_t must be affine too. Hence, a solution requires $\lambda_t = \Lambda_t r_t + \bar{\lambda}_t$ and $\xi_t = \Xi_t r_t + \bar{\xi}_t$, where

$$\begin{aligned}
\Lambda_t &\equiv -\gamma\sigma^2 \int_0^\infty \left(\alpha(\tau) [A_t(\tau)]^2 + \alpha^*(\tau) [A_t^*(\tau)]^2 \right) d\tau, \\
\bar{\lambda}_t &\equiv \gamma\sigma^2 \int_0^\infty \left[(S_t(\tau) - h_t(\tau) - \alpha(\tau) C_t(\tau)) A_t(\tau) + (S_t^*(\tau) - h_t^*(\tau) - \alpha^*(\tau) C_t^*(\tau)) A_t^*(\tau) \right] d\tau, \\
\Xi_t &\equiv -\gamma\psi_t\delta^2 \int_0^\infty \alpha(\tau) A_t(\tau) d\tau, \\
\bar{\xi}_t &\equiv \gamma\psi_t\delta^2 \int_0^\infty (S_t(\tau) - h_t(\tau) - \alpha(\tau) C_t(\tau)) d\tau,
\end{aligned}$$

where $\alpha(\tau) = \alpha/\tau$. With this notation, if we substitute $\mu_t(\tau)$ and $\mu_t^*(\tau)$ from (10)-(11) into (13)-(14), the first-order conditions on the arbitrageurs' portfolio weights are:

$$\begin{aligned}
0 = & -\left(\frac{\partial A_t}{\partial \tau} - \frac{\partial A_t}{\partial t} \right) r_t - \left(\frac{\partial C_t}{\partial \tau} - \frac{\partial C_t}{\partial t} \right) + A_t(\tau) \kappa(\bar{r} - r_t) - \frac{1}{2}\sigma^2 [A_t(\tau)]^2 + r_t \\
& + A_t(\tau) \left(\Lambda_t r_t + \bar{\lambda}_t \right) + \psi_t\delta + \left(\Xi_t r_t + \bar{\xi}_t \right),
\end{aligned}$$

and

$$\begin{aligned} 0 &= -\left(\frac{\partial A_t^*}{\partial \tau} - \frac{\partial A_t^*}{\partial t}\right) r_t - \left(\frac{\partial C_t^*}{\partial \tau} - \frac{\partial C_t^*}{\partial t}\right) + A_t^*(\tau)\,\kappa\,(\bar{r} - r_t) - \frac{1}{2}\sigma^2\left[A_t^*(\tau)\right]^2 + r_t \\ &+ A_t^*(\tau)\left(\Lambda_t r_t + \bar{\lambda}_t\right). \end{aligned}$$

Substituting in Λ_t, $\bar{\lambda}_t$, Ξ_t, and $\bar{\xi}_t$, and grouping the terms with and without r, we get

$$0 = -\frac{\partial A_t}{\partial \tau} + \frac{\partial A_t}{\partial t} - A_t(\tau)\,\kappa + 1 + \Lambda_t A_t(\tau) + \Xi_t. \tag{41}$$

$$0 = -\frac{\partial C_t}{\partial \tau} + \frac{\partial C_t}{\partial t} + A_t(\tau)\,\kappa\bar{r} - \frac{1}{2}\sigma^2\left[A_t(\tau)\right]^2 + \bar{\lambda}_t A_t(\tau) + \psi_t\delta + \bar{\xi}_t. \tag{42}$$

$$0 = -\frac{\partial A_t^*}{\partial \tau} + \frac{\partial A_t^*}{\partial t} - A_t^*(\tau)\,\kappa + 1 + \Lambda_t A_t^*(\tau) \tag{43}$$

$$0 = -\frac{\partial C_t^*}{\partial \tau} + \frac{\partial C_t^*}{\partial t} + A_t^*(\tau)\,\kappa\bar{r} - \frac{1}{2}\sigma^2\left[A_t^*(\tau)\right]^2 + \bar{\lambda}_t A_t^*(\tau). \tag{44}$$

This provides a system of PDEs to determine functions $(A_t(\tau), C_t(\tau))$ and $(A_t^*(\tau), C_t^*(\tau))$, verifying our guess that the bond price is an affine function of r_t.

A.3 Derivation of analytical results in Section 2.1

A.3.1 Proof of Proposition 1

We start with the definition of yields:

$$y_t(\tau) = -\frac{\log P_t(\tau)}{\tau},$$

and the fact that a bond with price $P_t(\tau)$ at time t will have a price equal to its face value, $P_{t+\tau}(0) = 1$, at time $t + \tau$:

$$0 = \log P_{t+\tau}(0) = \log P_t(\tau) + \mathbb{E}_t \int_0^\tau d \log P_{t+s}(\tau - s)\, ds.$$

Then, substituting for $P_t(\tau)$ in the definition of the yield, we have

$$
\begin{aligned}
y_t(\tau) &= \frac{1}{\tau}\mathbb{E}_t\int_0^\tau d\log P_{t+s}(\tau-s)\,ds = \frac{1}{\tau}\int_0^\tau \mathbb{E}_t\frac{dP_{t+s}(\tau-s)}{P_{t+s}(\tau-s)}ds \\
&= \frac{1}{\tau}\int_0^\tau \mathbb{E}_t\mu_{t+s}(\tau-s)ds \\
&= \underbrace{\frac{1}{\tau}\mathbb{E}_t\int_0^\tau r_{t+s}ds}_{\text{Expected rates } y_t^{EX}(\tau)} + \underbrace{\frac{1}{\tau}\mathbb{E}_t\int_0^\tau A_{t+s}(\tau-s)\lambda_{t+s}ds}_{\text{Term premium } y_t^{TP}(\tau)} \\
&+ \underbrace{\frac{1}{\tau}\mathbb{E}_t\int_0^\tau \delta\psi_{t+s}ds}_{\text{Expected default loss } y_t^{DL}(\tau)} + \underbrace{\frac{1}{\tau}\mathbb{E}_t\int_0^\tau \xi_{t+s}ds}_{\text{Credit risk premium } y_t^{CR}(\tau)},
\end{aligned}
$$

where the second line applies equation (9) and third line applies (13).

A.3.2 Details of Propositions 2-4

To derive the formulas on which Propositions 2, 3, and 4 are based, we start with the system of equations (41)-(44) from Appendix A.2. In steady state, the system simplifies to

$$
\begin{aligned}
0 &= -\frac{\partial A}{\partial\tau} - A(\tau)\kappa + 1 + \Lambda A(\tau) + \Xi. && (45)\\
0 &= -\frac{\partial C}{\partial\tau} + A(\tau)\kappa\bar{r} - \frac{1}{2}\sigma^2[A(\tau)]^2 + \bar{\lambda}A(\tau) + \psi\delta + \bar{\xi}. && (46)\\
0 &= -\frac{\partial A^*}{\partial\tau} - A^*(\tau)\kappa + 1 + \Lambda A^*(\tau) && (47)\\
0 &= -\frac{\partial C^*}{\partial\tau} + A^*(\tau)\kappa\bar{r} - \frac{1}{2}\sigma^2[A^*(\tau)]^2 + \bar{\lambda}A^*(\tau), && (48)
\end{aligned}
$$

where we have suppressed the time index as functions are time-invariant. Differential equations (45) and (47) can be solved as

$$
A^*(\tau) = \frac{1-e^{-\hat{\kappa}\tau}}{\hat{\kappa}},\ A(\tau) = \frac{(1+\Xi)\left(1-e^{-\hat{\kappa}\tau}\right)}{\hat{\kappa}}, \qquad (49)
$$

where

$$
\hat{\kappa} = \kappa - \Lambda = \kappa + \gamma\sigma^2\int_0^\infty\left(\alpha(\tau)\left(\frac{(1+\Xi)\left(1-e^{-\hat{\kappa}\tau}\right)}{\hat{\kappa}}\right)^2 + \alpha^*(\tau)\left(\frac{1-e^{-\hat{\kappa}\tau}}{\hat{\kappa}}\right)^2\right)d\tau.
$$

Then, integrating equations (46) and (48), we get

$$\begin{aligned} C^{*}(\tau) &= \int_{0}^{\tau}\left[A^{*}(u)\left(\kappa\bar{r}+\bar{\lambda}\right)-\frac{1}{2}\sigma^{2}\left[A^{*}(u)\right]^{2}\right]du, \\ C(\tau) &= \left(\psi\delta+\bar{\xi}\right)\tau+\int_{0}^{\tau}\left[A(u)\left(\kappa\bar{r}+\bar{\lambda}\right)-\frac{1}{2}\sigma^{2}\left[A(u)\right]^{2}\right]du. \end{aligned}$$

Next, we analyze the limit as maturity converges to zero:

$$\begin{aligned} \lim_{\tau\to 0} y_{t}(\tau) &= \left(\psi\delta+\bar{\xi}\right)+\lim_{\tau\to 0}\left[\frac{(1+\Xi)\left(1-e^{-\hat{\kappa}\tau}\right)}{\hat{\kappa}}r_{t}+A(\tau)\left(\kappa\bar{r}+\bar{\lambda}\right)-\frac{1}{2}\sigma^{2}\left[A(\tau)\right]^{2}\right] \\ &= (1+\Xi)\,r_{t}+\left(\psi\delta+\bar{\xi}\right). \end{aligned}$$

Here we have used L'Hôpital's rule to obtain

$$\lim_{\tau\to 0}\frac{(1+\Xi)\left(1-e^{-\hat{\kappa}\tau}\right)}{\hat{\kappa}\tau}=\lim_{\tau\to 0}\frac{(1+\Xi)\,\hat{\kappa}e^{-\hat{\kappa}\tau}}{\hat{\kappa}}=(1+\Xi),$$

and the fact that $A(0)=0$ to derive

$$\lim_{\tau\to 0}\frac{\int_{0}^{\tau}\left[A(u)\left(\kappa\bar{r}+\bar{\lambda}\right)-\frac{1}{2}\sigma^{2}\left[A(u)\right]^{2}\right]du}{\tau} = \lim_{\tau\to 0}A(\tau)\left(\kappa\bar{r}+\bar{\lambda}\right)-\tfrac{1}{2}\sigma^{2}\left[A(\tau)\right]^{2} = 0.$$

B Appendix: Robustness exercises

This appendix presents two alternative calibrations that illustrate the robustness of our results. Different calibration procedures change the estimated parameters, but preserve the main theoretical and policy conclusions. We consistently find that sovereign risk can explain large yield curve shifts, including at short maturities, and that default risk extraction is the most important transmission channel of asset purchases. As long as the model is calibrated to match the observed impact of the PEPP announcement, the policy comparison across alternative purchase designs is quantitatively similar.

Alternative calibration: steady state. Our benchmark calibration supposes that the effective lower bound period was a prolonged, low-probability deviation from typical euro area yields, and takes account of fiscal forecasts looking forward from that time. An alternative is simply to assume that the effective lower bound period represented fluctuations around a steady state of the model (possibly one of several

conditional steady states), and calibrate accordingly. This alternative assumption leads us to calibrate the mean and standard deviation of the risk-free rate to their sample values, $r_{elb} = -49$bp and $\sigma_{elb} = 32$bp. Similarly, fiscal variables are assumed constant, equal to at their mean values from 2013-2019. We must then reestimate the parameters γ, ψ_{ss}, and θ (we use the subscript "ss" to indicate the steady state value of the default probability, and define the default probability function around the intercept ψ_{ss}). Fig. 11 shows the resulting steady-state yield curve for Italy.

Figure 11: Robustness: steady state calibration

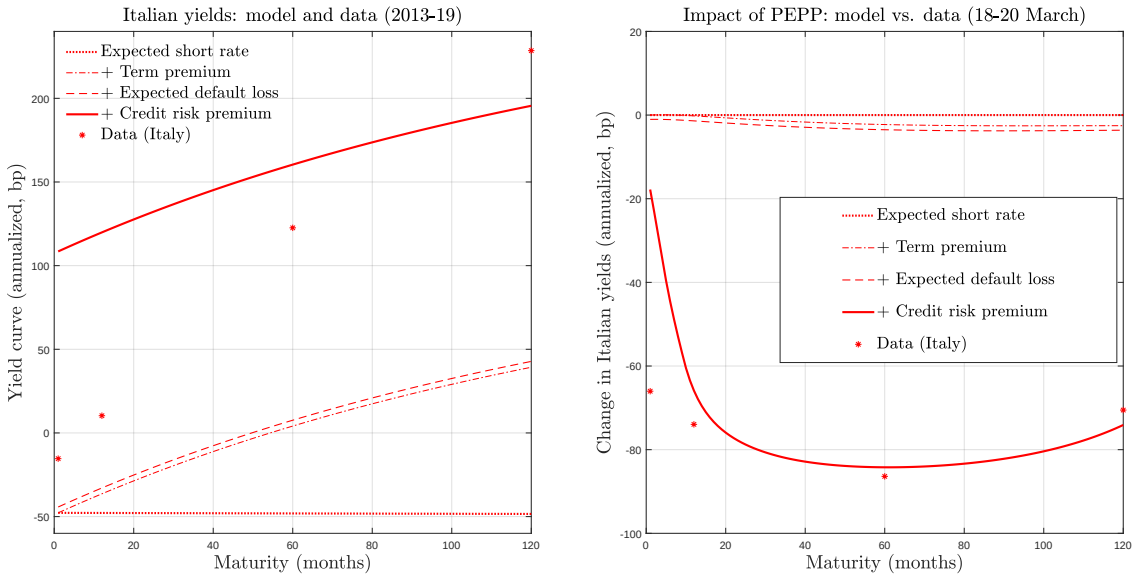

Notes. This figure shows the results of a calibration that treats the ELB period as a steady state of the model. The values of γ, ψ_{ss}, and θ are recalibrated to match the German term premium, the Italian sovereign spread, and the impact of PEPP on Italian yields.
Left panel. Italian steady state yield curve decomposition. Red lines: steady state yields (model). Red stars: Italian yields, 2013-2019 (from Datastream).
Right panel. Shift in Italian yields from 18 March 2020 (before PEPP) to 20 March 2020 (after). Red lines: model. Red stars: Data (from Datastream)

On the left, we show the steady-state yield curve for Italy. The red lines decompose the model-generated yield curve; the red stars are the mean yields from 2013-2019. In this case, the expectations term is simply a flat line at $y_{ss}^{EX}(\tau) = -49$bp, since yields are expected to remain at their steady state value. Hence, compared to our benchmark calibration, this alternative infers a larger steady state term premium – 104bp for ten-year bonds – that fully accounts for the slope of the German yield curve. On top of these terms, the default-related terms $y_{ss}^{DL}(\tau)$ and $y_{ss}^{CR}(\tau)$ are almost constant

across maturities. This occurs because fiscal variables are assumed constant in this steady state, which implies that the sovereign premium does not vary with maturity. In contrast, our benchmark calibration strategy infers that fiscal pressure is expected to increase over time, so the sovereign premium increases with maturity, better matching the data.

In the right panel, we see the impact of PEPP under this specification, which is almost identical to our benchmark results. Since this calibration requires higher risk aversion (to match a higher term premium than that in our benchmark calibration), a smaller change in the default probability suffices to match the Italian yield curve shift after the PEPP announcement. Hence we see a slightly smaller change in the expected default premium $y_t^{DL}(\tau)$ than we observed under the benchmark parameters (compare Figure 3). But this is hardly noticeable, since again the vast majority of the decrease in yields is explained by a fall in the credit risk premium $y_t^{CR}(\tau)$. Likewise, the comparison across more and less flexible asset purchase designs (not shown, available on request) is virtually identical to the results reported in Sec. 5. Thus, while this alternative calibration procedure is less successful at matching data from the ELB period, the resulting policy analysis is essentially the same as in our benchmark results.

Alternative calibration: Germany and Spain. Our main results were calibrated to describe a union made up of Germany and Italy. PEPP had especially strong effects on Italian yields, since Italy has a large outstanding stock of sovereign bonds, and faces a high sovereign premium. Nonetheless, a simple recalibration shows that our model also fits well for a union consisting of Germany and Spain. Since Spain has less debt than Italy, a higher risk aversion parameter, $\gamma = 0.14$, is needed to match the German term premium in this case. The probability parameters are quite similar to those of the German and Italian calibration, with $\psi_{elb} = 0.0009$ and $\theta = 5.04 * 10^{-5}$.

The main results are shown in Fig. 12. The left panel compares the model-generated decomposition of the Spanish yield curve to average Spanish yields over 2013-2019. As in the case of Italy, fiscal forecasts predict increasing fiscal pressure over the ELB period, resulting in sovereign spreads that increase with maturity. The right panel shows the shift in Spanish yields when PEPP was announced, in the model (red lines) and data (stars). Since Spain has a lower debt-to-GDP ratio than Italy, its steady state sovereign premium and the effects of PEPP are smaller for Spain than they are for Italy, but model fit is very similar when mapping either country to Periphery. Results for Germany (not shown) are almost identical to those seen in Figs. 2 and 3.

Figure 12: Modelling Germany and Spain

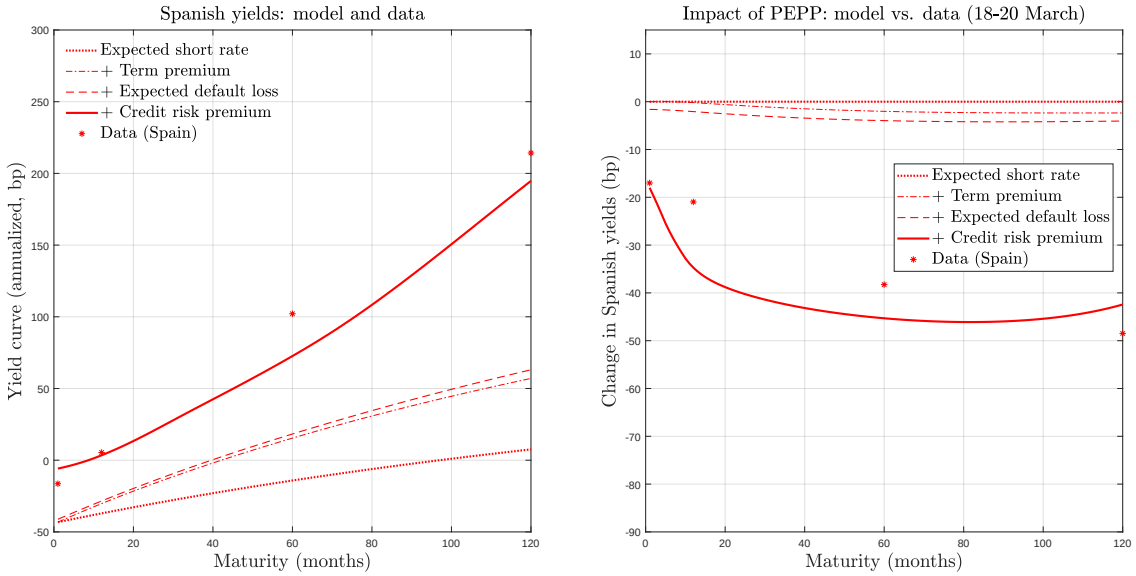

Notes. This figure shows the results of applying our model to a monetary union consisting of Germany and Spain. The values of γ, ψ_{elb}, and θ are recalibrated to match the German term premium, the Spanish sovereign spread, and the impact of PEPP on Spanish yields.
Left panel. Spanish yield curve decomposition. Red lines: steady state yields (model). Red stars: Spanish yields, 2013-2019 (from Datastream).
Right panel. Shift in Spanish yields from 18 March 2020 (before PEPP) to 20 March 2020 (after). Red lines: model decomposition of shift in yield curve. Red stars: Data (from Datastream).

Internet Appendix

C Appendix: Computing the solution

C.1 Numerical algorithm: continuous time

C.1.1 Finite-difference computation of the stochastic steady state

The stochastic steady state of our model must satisfy the system of ODEs (45)-(48). These can be solved by a finite difference method.[46] To do so, we consider a grid of maturities $(\tau_1, .., \tau_I)$ with $\tau_0 = 0$ and constant step size $\Delta\tau$, so that $\tau_i \equiv \tau(i) = i\Delta\tau$. Define

$$\begin{aligned} A_i &= A(\tau_i), A_i^* = A^*(\tau_i), C_i = C(\tau_i), C_i^* = C^*(\tau_i), \\ S_i &= S(\tau_i), S_i^* = S^*(\tau_i), \alpha_i = \alpha(\tau_i), \alpha_i^* = \alpha^*(\tau_i), \\ h &= h(\tau_i), h_i^* = h^*(\tau_i). \end{aligned}$$

The boundary conditions are $A_0 = A(0) = 0$ and $C_0 = C(0) = 0$ because an instantaneous bond trades at par. We begin with a guess of A_i^n, A_i^{n*}, with $n = 0$. For instance, we can begin with $A_i^n = A_i^{n*} = \tau_i$ and $C_i^n = C_i^{n*} = 0$. Then, considering a backward finite-difference approximation $\frac{\partial A^{n+1}(\tau(i))}{\partial\tau} \approx \frac{A_i^{n+1} - A_{i-1}^{n+1}}{\Delta\tau}$, and likewise for the other unknown functions, we approximate the ODEs as:

$$\begin{aligned} \frac{A_i^{n+1} - A_{i-1}^{n+1}}{\Delta\tau} &= A_i^{n+1}\Lambda^n - A_i^{n+1}\kappa + 1 + \Xi^n, \\ \frac{C_i^{n+1} - C_{i-1}^{n+1}}{\Delta\tau} &= A_i^{n+1}\bar{\lambda}^n + A_i^{n+1}\kappa\bar{r} - \frac{1}{2}\sigma^2\left[A_i^{n+1}\right]^2 + \psi_{ss}\delta + \bar{\xi}^n, \\ \frac{A_i^{(n+1)*} - A_{i-1}^{(n+1)*}}{\Delta\tau} &= A_i^{(n+1)*}\Lambda^n - A_i^{(n+1)*}\kappa + 1, \\ \frac{C_i^{(n+1)*} - C_{i-1}^{(n+1)*}}{\Delta\tau} &= A_i^{(n+1)*}\bar{\lambda}^n + A_i^{(n+1)*}\kappa\bar{r} - \frac{1}{2}\sigma^2\left[A_i^{(n+1)*}\right]^2, \end{aligned}$$

[46] We have defined and computed both continuous-time and discrete-time versions of the model. The discrete time version is described in the next section. Numerical simulations of both versions give the same results.

where

$$
\begin{aligned}
\Lambda^n &= -\gamma\sigma^2 \sum_{i=1}^{I} \left(\alpha_i \left[A_i^n\right]^2 + \alpha_i^* \left[A_i^{n*}\right]^2\right) \Delta\tau, \\
\bar{\lambda}^n &= \gamma\sigma^2 \sum_{i=1}^{I} \left[\left(S_i - h_i - \alpha_i C_i^n\right) A_i^n + \left(S_i^* - h_i^* - \alpha_i^* C^{n*}\right) A_i^{n*}\right] \Delta\tau, \\
\Xi^n &= -\gamma\psi_{ss}\delta^2 \sum_{i=1}^{I} \alpha_i A_i^n \Delta\tau. \\
\xi^n &= \gamma\psi_{ss}\delta^2 \sum_{i=1}^{I} \left[\left(S_i - h_i - \alpha_i C_i^n\right)\right] \Delta\tau.
\end{aligned}
$$

In matrix form, this amounts to

$$
\overbrace{\begin{bmatrix}
\frac{1}{\Delta\tau} - \Lambda^n + \kappa & 0 & 0 & \cdots & 0 \\
-\frac{1}{\Delta\tau} & \frac{1}{\Delta\tau} - \Lambda^n + \kappa & 0 & \cdots & 0 \\
\vdots & -\frac{1}{\Delta\tau} & \frac{1}{\Delta\tau} - \Lambda^n + \kappa & \cdots & \vdots \\
0 & 0 & \cdots & \ddots & 0 \\
0 & 0 & \cdots & -\frac{1}{\Delta\tau} & \frac{1}{\Delta\tau} - \Lambda^n + \kappa
\end{bmatrix}}^{\mathbf{F^n}}
\overbrace{\begin{bmatrix} A_1^{n+1} \\ A_2^{n+1} \\ \vdots \\ A_{I-1}^{n+1} \\ A_I^{n+1} \end{bmatrix}}^{\mathbf{A^{n+1}}}
= \overbrace{\begin{bmatrix} 1+\Xi^n \\ 1+\Xi^n \\ \vdots \\ 1+\Xi^n \\ 1+\Xi^n \end{bmatrix}}^{\mathbf{f^n}}, \tag{50}
$$

$$
\begin{bmatrix}
\frac{1}{\Delta\tau} - \Lambda^n + \kappa & 0 & 0 & \cdots & 0 \\
-\frac{1}{\Delta\tau} & \frac{1}{\Delta\tau} - \Lambda^n + \kappa & 0 & \cdots & 0 \\
\vdots & -\frac{1}{\Delta\tau} & \frac{1}{\Delta\tau} - \Lambda^n + \kappa & \cdots & \vdots \\
0 & 0 & \cdots & \ddots & 0 \\
0 & 0 & \cdots & -\frac{1}{\Delta\tau} & \frac{1}{\Delta\tau} - \Lambda^n + \kappa
\end{bmatrix}
\overbrace{\begin{bmatrix} A_1^{(n+1)*} \\ A_2^{(n+1)*} \\ \vdots \\ A_{I-1}^{(n+1)*} \\ A_I^{(n+1)*} \end{bmatrix}}^{\mathbf{A^{(n+1)*}}}
= \overbrace{\begin{bmatrix} 1 \\ 1 \\ \vdots \\ 1 \\ 1 \end{bmatrix}}^{\mathbf{f^*}}, \tag{51}
$$

$$
\overbrace{\begin{bmatrix}
\frac{1}{\Delta\tau} & 0 & 0 & \cdots & 0 \\
-\frac{1}{\Delta\tau} & \frac{1}{\Delta\tau} & 0 & \cdots & 0 \\
\vdots & -\frac{1}{\Delta\tau} & \frac{1}{\Delta\tau} & \cdots & \vdots \\
0 & 0 & \cdots & \ddots & 0 \\
0 & 0 & \cdots & -\frac{1}{\Delta\tau} & \frac{1}{\Delta\tau}
\end{bmatrix}}^{\mathbf{G}}
\overbrace{\begin{bmatrix} C_1^{n+1} \\ C_2^{n+1} \\ \vdots \\ C_{I-1}^{n+1} \\ C_I^{n+1} \end{bmatrix}}^{\mathbf{C^{n+1}}}
= \overbrace{\begin{bmatrix}
A_1^{n+1}\bar{\lambda}^n + A_1^{n+1}\kappa\bar{r} - \frac{1}{2}\sigma^2\left[A_1^{n+1}\right]^2 + \psi_{ss}\delta + \bar{\xi}^n \\
A_2^{n+1}\bar{\lambda}^n + A_2^{n+1}\kappa\bar{r} - \frac{1}{2}\sigma^2\left[A_2^{n+1}\right]^2 + \psi_{ss}\delta + \bar{\xi}^n \\
\vdots \\
A_{I-1}^{n+1}\bar{\lambda}^n + A_{I-1}^{n+1}\kappa\bar{r} - \frac{1}{2}\sigma^2\left[A_{I-1}^{n+1}\right]^2 + \psi_{ss}\delta + \bar{\xi}^n \\
A_I^{n+1}\bar{\lambda}^n + A_I^{n+1}\kappa\bar{r} - \frac{1}{2}\sigma^2\left[A_I^{n+1}\right]^2 + \psi_{ss}\delta + \bar{\xi}^n
\end{bmatrix}}^{\mathbf{g^{n+1}}}, \tag{52}
$$

$$\begin{bmatrix} \frac{1}{\Delta\tau} & 0 & 0 & \cdots & 0 \\ -\frac{1}{\Delta\tau} & \frac{1}{\Delta\tau} & 0 & \cdots & 0 \\ \vdots & -\frac{1}{\Delta\tau} & \frac{1}{\Delta\tau} & \cdots & \vdots \\ 0 & 0 & \cdots & \ddots & 0 \\ 0 & 0 & \cdots & -\frac{1}{\Delta\tau} & \frac{1}{\Delta\tau} \end{bmatrix} \overbrace{\begin{bmatrix} C_1^{(n+1)*} \\ C_2^{(n+1)*} \\ \vdots \\ C_{I-1}^{(n+1)*} \\ C_I^{(n+1)*} \end{bmatrix}}^{\mathbf{C}^{(\mathbf{n+1})*}} = \overbrace{\begin{bmatrix} A_1^{(n+1)*}\bar{\lambda}^n + A_1^{(n+1)*}\kappa\bar{r} - \frac{1}{2}\sigma^2\left[A_1^{(n+1)*}\right]^2 \\ A_2^{(n+1)*}\bar{\lambda}^n + A_2^{(n+1)*}\kappa\bar{r} - \frac{1}{2}\sigma^2\left[A_2^{(n+1)*}\right]^2 \\ \vdots \\ A_{I-1}^{(n+1)*}\bar{\lambda}^n + A_{I-1}^{(n+1)*}\kappa\bar{r} - \frac{1}{2}\sigma^2\left[A_{I-1}^{(n+1)*}\right]^2 \\ A_I^{(n+1)*}\bar{\lambda}^n + A_I^{(n+1)*}\kappa\bar{r} - \frac{1}{2}\sigma^2\left[A_I^{(n+1)*}\right]^2 \end{bmatrix}}^{\mathbf{g}^{(\mathbf{n+1})*}}, \tag{53}$$

where we have already applied the boundary conditions.

The idea is to solve equations (50) and (51) iteratively from the initial guess, updating Λ^n and Ξ^n and at each step, and then calculate $\bar{\lambda}^n$ and $\bar{\xi}^n$ in order to solve (52) and (53) in a single step.

C.1.2 Computation of the dynamics

To compute the dynamics, consider a distant terminal time T at which the model has converged to its steady state. We solve the PDEs (41)-(44) backwards from time T with time steps of size $\Delta t \equiv \Delta\tau$, so that backwards induction step n refers to calendar time $t(n) \equiv T - n\Delta\tau$. Using the fact that $A_i^{n+1} - A_i^n \approx -\frac{\partial A^n(\tau(i))}{\partial t}\Delta\tau$, the PDEs can be discretized as follows::

$$\begin{aligned} \frac{\mathbf{A}^{\mathrm{n+1}} - \mathbf{A}^{\mathrm{n}}}{\Delta\tau} + \mathbf{F}^{\mathrm{n}}\mathbf{A}^{\mathrm{n}} &= \mathbf{f}^{\mathrm{n}}, \\ \frac{\mathbf{A}^{(\mathrm{n+1})*} - \mathbf{A}^{\mathbf{n}*}}{\Delta\tau} + \mathbf{F}^{\mathbf{n}}\mathbf{A}^{\mathrm{n}*} &= \mathbf{f}^{*}, \\ \frac{\mathbf{C}^{\mathrm{n+1}} - \mathbf{C}^{\mathrm{n}}}{\Delta\tau} + \mathbf{G}\mathbf{C}^{\mathrm{n}} &= \mathbf{g}^{\mathrm{n}}, \\ \frac{\mathbf{C}^{(\mathrm{n+1})*} - \mathbf{C}^{\mathrm{n}*}}{\Delta\tau} + \mathbf{G}\mathbf{C}^{\mathrm{n}*} &= \mathbf{g}^{\mathrm{n}*}. \end{aligned}$$

Matrices $\mathbf{F}^{\mathrm{n}}$, $\mathbf{G}$, $\mathbf{f}^{\mathrm{n}}$, $\mathbf{f}^{*}$, $\mathbf{g}^{\mathrm{n}}$, and $\mathbf{g}^{\mathrm{n}*}$ are defined as before, except that we calculate Λ_t, Ξ_t, $\bar{\lambda}_t$, and $\bar{\xi}_t$ under time-varying conditions. In particular, we evaluate them conditional on the net bond supply $S_t(\tau)$ and default probability ψ_t at time $t = t(n)$.[47]

[47] Inspecting the definitions of the matrices in (50)-(53), we can see that this algorithm calculates equilibrium objects at time $t(n) - \Delta\tau$ using the risk prices $\lambda_{t(n)}$ and $\xi_{t(n)}$ from time $t(n)$. It would therefore be incorrect to apply this algorithm with a large time step $\Delta\tau$, but in the limit as $\Delta\tau \to 0$, it gives the correct solution of the continuous-time PDE.

C.2 Discrete time representation

It is straightforward to derive and compute a discrete-time framework that is equivalent to our continuous-time model. In discrete time, we write the price of a bond with a maturity of i periods, issued by jurisdiction $j \in \{P, C\}$ ("Periphery" or "Core"), as $P_{i,t}^j = \exp\left(p_{i,t}^j\right) = \exp\left(-A_{i,t}^j r_t - C_{i,t}^j\right)$. Let the rate on reserves follow $r_{t+1} = \rho r_t + (1-\rho)\bar{r} + \sigma\varepsilon_{t+1}$, where $\varepsilon_{t+1} \sim N(0,1)$. If arbitrageurs maximize a mean-variance utility function over the increase of their wealth, then if the time period is sufficiently short, their optimization problem can be approximated as follows:[48]

$$\begin{aligned}\max_{\{X_{i,t}^j\}} \quad & \left(W_t - \textstyle\sum_{i=1}^I \sum_{j\in\{P,C\}} X_{i,t}^j\right) r_t \\ + \quad & \textstyle\sum_{i=1}^I \sum_{j\in\{P,C\}} X_{i,t}^j \left(-C_{i-1,t+1}^j - A_{i-1,t+1}^j\left((1-\rho)\bar{r} + \rho r_t\right) + C_{i,t}^j + A_{i,t}^j r_t + \frac{\sigma^2}{2}\left(A_{i-t,t+1}^j\right)^2 - \delta\psi_t^j\right) \\ - \quad & \frac{\gamma\sigma^2}{2}\left[\textstyle\sum_{i=2}^I \sum_{j\in\{P,C\}} X_{i,t}^j A_{i-1,t+1}^j\right]^2 - \frac{\gamma\psi_t^P}{2}\delta^2\left[\textstyle\sum_{i=1}^I X_{i,t}^P\right]^2 .\end{aligned}$$

where $\psi_t^C = 0$ denotes the Core default probability, and $\psi_t^P = \psi_t$ is the Peripheral default probability, given by (35). Hence, the first-order condition on the investment $X_{i,t}^j$ in bonds of maturity i from jurisdiction j is

$$r_t = -\left(C_{i-1,t+1}^j + A_{i-1,t+1}^j\left((1-\rho)\bar{r} + \rho r_t\right)\right) + \left(C_{i,t}^j + A_{i,t}^j r_t\right) + \frac{\sigma^2}{2}\left(A_{i-t,t+1}^j\right)^2 - \delta\psi_t^j - A_{i-1,t+1}^j\lambda_t - \xi_t^j,$$

where

$$\lambda_t = \gamma\sigma^2\left[\sum_{i=2}^I \sum_{j\in\{P,C\}} X_{i,t}^j A_{i-1,t+1}^j\right],$$

$$\xi_t^j = \gamma\psi_t^j\delta^2\sum_{i=1}^I X_{i,t}^j .$$

Note that since $A_{0,t}^j = C_{0,t}^j = 0$, the first-order condition for holdings of one-period Core bonds is simply

$$r_t = y_{1,t}^C = C_{i,t}^j + A_{i,t}^j r_t ,$$

[48] See Hamilton and Wu (2012) for details.

and the FOC for longer bonds can be interpreted as

$$p_{i,t}^j = -r_t + E_t p_{i-1,t+1}^j + \frac{1}{2} Var_t p_{i-1,t+1}^j - A_{i-1,t+1}^j \lambda_t - \delta \psi_t^j - \xi_t^j,$$

or equivalently

$$P_{i,t}^j = \exp\left(-r_t - A_{i-1,t+1}^j \lambda_t - \delta \psi_t^j - \xi_t^j\right) E_t P_{i-1,t+1}^j.$$

We now apply the market clearing condition $X_{i,t}^j = S_{i,t}^j - Z_{i,t}^j$, where preferred-habitat demand is $Z_{i,t}^j = h_{i,t}^j - \alpha_i^j p_{i,t}^j$, and we write the risk compensation terms in affine form as $\lambda_t = \Lambda_t r_t + \bar{\lambda}_t$ and $\xi_t^P = \Xi_t^P r_t + \bar{\xi}_t^P$, with $\xi_t^C = \Xi_t^C = \bar{\xi}_t^C = 0$. Then, the first-order conditions imply the following restrictions on the affine pricing coefficients:

$$A_{i,t}^j = A_{1,t}^C + A_{i-1,t+1}^j (\rho + \Lambda_t) + \Xi_t^j, \tag{54}$$

$$C_{i,t}^j = C_{1,t}^C + C_{i-1,t+1}^j - \frac{1}{2}\left(\sigma A_{i-1,t+1}^j\right)^2 + A_{i-1,t+1}^j \left((1-\rho)\bar{r} + \bar{\lambda}_t\right) + \delta \psi_t + \bar{\xi}_t^j, \tag{55}$$

where

$$\Lambda_t = -\gamma \sigma^2 \sum_{i=2}^{I} \sum_{j \in \{P,C\}} A_{i-1,t+1}^j \left(\alpha_i^j A_i^j\right), \tag{56}$$

$$\bar{\lambda}_t = \gamma \sigma^2 \sum_{i=2}^{I} \sum_{j \in \{P,C\}} A_{i-1,t+1}^j \left(S_{i,t}^j - h_{i,t}^j - \alpha_i^j C_i^j\right), \tag{57}$$

$$\Xi_t^P = -\gamma \delta^2 \psi_t^P \sum_{i=1}^{I} \left(\alpha_i^P A_i^P\right), \tag{58}$$

$$\bar{\xi}_t^P = \gamma \delta^2 \psi_t^P \sum_{i=1}^{I} \left(S_{i,t}^P - h_{i,t}^P - \alpha_i^P C_i^P\right). \tag{59}$$

These difference equations can be solved by backwards induction, starting from a distant time T at which we assume that the pricing functions are known, bearing in mind that $A_{0,t}^j = C_{0,t}^j = 0$ for all j and t. To ensure a correct solution of the discrete-time model, we can apply a fixed-point calculation at each time step:

1. Guess $A_{i,t}^j = A_{i,t+1}^j$ and $C_{i,t}^j = C_{i,t+1}^j$.
2. Calculate Λ_t, Ξ_t^P, $\bar{\lambda}_t$, and $\bar{\xi}_t^P$ from (56)-(59).

3. Update $A_{i,t}^j = A_{i,t+1}^j$ and $C_{i,t}^j = C_{i,t+1}^j$ using (54)-(55).

4. Iterate to convergence.

Once the time t equilibrium has been calculated, we can step backwards to calculate the time $t-1$ equilibrium by the same method.